Supporting Information

Geospatial Life Cycle Analysis of Greenhouse Gas Emissions from US Liquefied Natural Gas Supply Chains

Yuanrui Zhu[1,2], David T. Allen[1,3], and Arvind P. Ravikumar[1,2*]

[1]Energy Emissions Modeling and Data Lab (EEMDL), The University of Texas at Austin, Austin TX 78712
[2]Department of Petroleum and Geosystems Engineering, The University of Texas at Austin, Austin TX 78712
[3]Department of Chemical Engineering, The University of Texas at Austin, Austin TX 78712

*Corresponding email: arvind.ravikumar@austin.utexas.edu

- Total number of pages: 53
- Total number of figures: 8
- Total number of tables: 40

Table of Contents

S 1. Model structure

Liquefied natural gas (LNG) supply chain includes serval stages from production through shipping, as shown in Figure S1. In this study, major supply chain stages include production, gathering and boosting (G&B), processing, transmission, liquefaction, and shipping. In our study we assume that upstream includes all processes from production and G&B stages. This definition of upstream emissions also enables the direct use of top-down methane emissions measurements within a lifecycle emissions inventory as co-location production and G&B facilities result in aggregate emissions measurements.

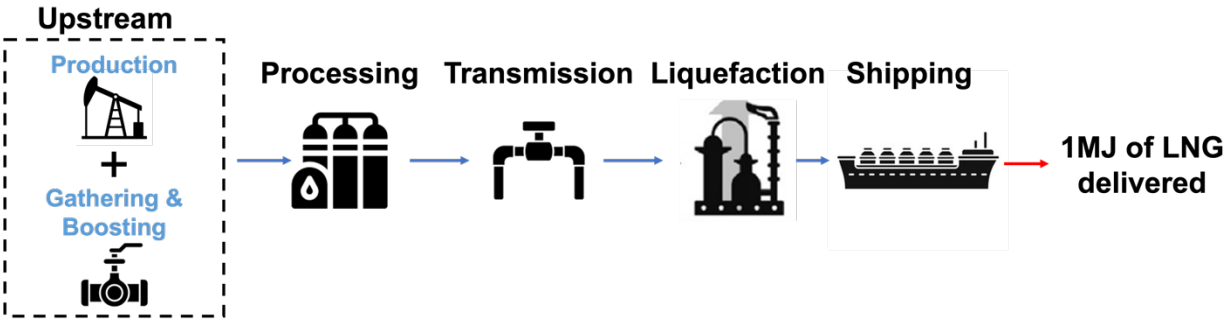

Figure S1. Major LNG supply chain stages included in this study: upstream that includes both production and G&B stages, processing, transmission, liquefaction, and shipping.

We design four LNG supply chains, with the NG produced in the Marcellus and Permian basins, transported, and then liquefied in the Sabine Pass Liquefaction (SPL) terminal, finally shipped to UK and China. For the Marcellus basin, natural gas is concentrated in the northeastern and southwestern Pennsylvania. The gas produced in the southwestern tends to be wet (primarily composed of methane and also include ethane, propane, butane and pentane), while most of the gas in the northeastern is dry (almost pure methane).[1] In our study, we selected the northeastern Marcellus as the study region and assume all natural gas in Marcellus sourced LNG supply chain are produced in this region. The upstream inventory data are derived from oil and gas operators or published literature that are specific to the study region.[2–5] The measurements methane emission rate is obtained from a recent measurement campaign conducted in northeastern Marcellus.[6] The produced gas, crude oil, and lease condensate production is obtained from the Pennsylvania Department of Environmental Protection, which is aggregated across all counties in the dry gas region.[7] However, the Permian basin produces both crude oil and NG across the whole basin. We selected the whole Permian basin as study region. The upstream inventory data for the Permian basin are derived from published reports[3], representing the average of whole basin. In addition, the employed measured methane emission

rate is obtained from a measurement campaign that covers the whole basin.[8] The production data of all co-products in that region is obtained from Texas railroad commission and New Mexico Oil Conservation Division.[9–12] The selection of northeastern Marcellus and Permian basin exemplify a wide range of NG production scenarios.

Figure S2 shows the model structure for the lifecycle assessment in this study. For each LNG supply chain, the emission intensity in the unit of gCO_2e/MJ stage throughput of each process is multiplied by stage throughput, and the allocation factor to estimate the energy allocated GHG emission of this process, and then the emissions from all processes are aggerated to obtain the total GHG emissions of the specific supply chain. In our model, the methane emission intensity is established by replacing inventory-based estimates with top-down measurements. The inventory-based methane emission intensities are calculated by aggregating all bottom-up process-based methane emission estimates across all stages of LNG supply chain. The top-down methane measurements are incorporated into our model by replacing inventory-based methane emission intensity with measurement-informed methane emission intensities. Natural gas stage throughput is the energy content of the gas entering each stage given 1MJ of LNG delivered to the destination calculated based on the energy conservation law. The allocation factor is calculated based on the production data of each product, which aims to distribute the emission among dry gas and other co-products. Finally, we obtain the GHG emission values for each LNG supply chain and compare with other peer-reviewed literature on the LCA of LNG supply chains.

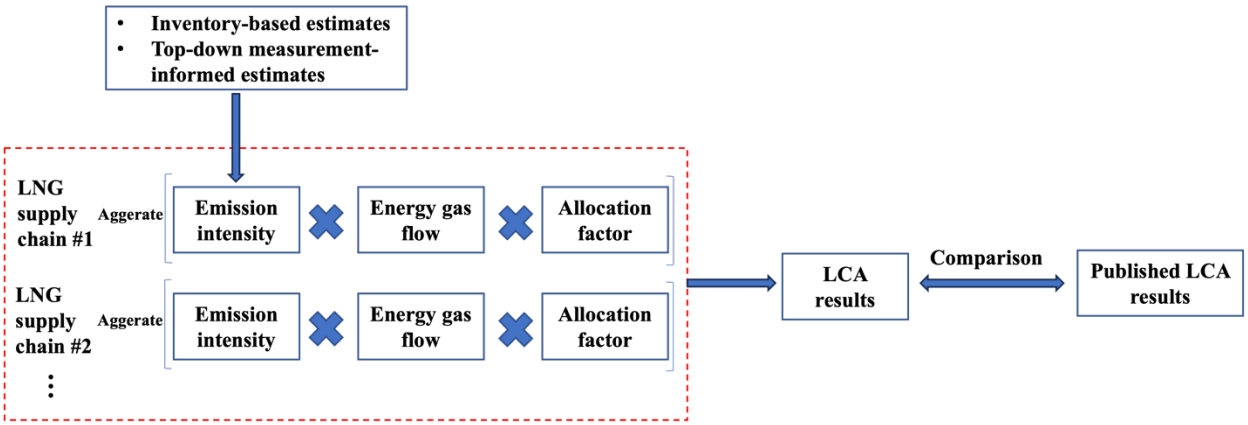

Figure S2. Model structure

S 2. Upstream production, gathering and boosting emission inventory

In this stage, the carbon dioxide emissions in both Marcellus and Permian basin come from diesel combustion for pre-production activities, fuel gas combustion for compression and dehydration, and flaring.

In the Marcellus basin, the volume of diesel used for drilling and fracturing, the volume of wastewater transported to be disposed come from operational data in that region, available from peer-reviewed studies[2]. Apart from diesel consumption, 2.32% of the produced natural gas is combusted to power compression, dehydration, and other operations, and 0.19 MMscf/well of the flow back gas is flared based on operations data in Marcellus region[2].

For the carbon dioxide emissions in the Permian basin, since the public data on pre-production activities were not available, we employed the same data as the Marcellus basin. Given the small contribution from diesel combustion during pre-production activities, this is not expected to impact the overall lifecycle emissions intensity. In addition, the raw data regarding the compression, dehydration and flaring operations were not available, so we used the Permian specific emission intensity of compression and other operations from the NETL report instead[3].

Methane emission estimates in the Marcellus basin are obtained by aggregating data from several sources, including official inventory estimates, peer-reviewed studies, and other reports. When calculating inventory-based emissions, the emission data from direct operational data and measurements are prioritized. For example, the volume of flowback gas and duration of gas unloading is based on publicly available operational data[2] and the emissions from pneumatic controllers at the wellhead and equipment leaks from the upstream facility are based on the published direct measurement results in the Appalachian region[5]. When the actual operation data and direct measurements data are not available, we use emissions data from published NETL reports[3,4]. When calculating measurement informed emission estimates, the measured methane emission rate are obtained from a recent published studies[6].

For the methane emissions in Permian basin, we use the emission data from NETL report[3] for calculating inventory based emission estimates and incorporates measured methane emission rate from recent published peer-reviewed studies[8,12].

S 2.1 Marcellus basin

Carbon dioxide

In the upstream stage, the carbon dioxide emission mainly comes from fuel combustion in the pre-production process, natural gas compression, natural gas dehydration, and flaring.

Carbon dioxide emissions from pre-production: All pre-production processes are powered by the combustion of diesel. The parameters used in pre-production processes are shown in Table S1.

Table S1. Parameters for pre-production processes

Parameters	Value	Unit	Data source
Gas estimated ultimate recovery	5.12	Bcf/well	Mallapragada et al., (2018)[2]
Diesel used for drilling	16,952	gal/well	Mallapragada et al., (2018)[2]
Diesel used for hydraulic fracturing	41,235	gal/well	Mallapragada et al., (2018)[2]
Diesel used for wastewater transport	969	Btu/ton/mile	OPGEE_v2.0[13]
Water used for hydraulic fracturing	245,293	bbl/well	Mallapragada et al., (2018)[2]
Distance from well to disposal site	352	miles	Laurenzi et al., (2013)[14]

The emission intensity for the pre-production processes is given by:

$$EI_{\text{upstream-diesel use},CO_2} = \frac{(Total\ diesel\ consumption\ per\ well)(Emission\ factor\ of\ diesel\ combustion)}{(Gas\ estimated\ ultimate\ recovery)}$$

$$= \frac{\left\{\left((16952+41235)\frac{gal}{well}\right)\left(139000\frac{Btu}{gal}\right)+\left(969\frac{Btu}{ton\cdot mile}\right)(352miles)\left(245293\frac{bbl}{well}\right)\left(0.159\frac{ton}{bbl}\right)\right\}\left(69.21\frac{gCO_2}{MJ}\right)\left(0.00105\frac{MJ}{Btu}\right)}{\left(5.12\frac{Bcf}{well}\right)\left(10^9\frac{scf}{Bcf}\right)\left(1023.1\frac{Btu}{scf}\right)\left(0.00105\frac{MJ}{Btu}\right)}$$

$$= 0.2836\ gCO_2/MJ \quad \text{(S1)}$$

Carbon dioxide emissions from compression and dehydration: The produced natural gas in the Marcellus basin is then compressed and dehydrated. The percentage of produced natural gas combusted to power these processes is obtained from peer-reviewed studies, where 2.2% of the produced natural gas is used for compression, while 0.12% is for dehydration and other operations[2]. The emission intensity for compression is given by:

$$EI_{\text{upstream-compression},CO_2} = (Percentage\ of\ NG\ combsuted\ for\ compression) \times (Emission\ facotr\ of\ NG\ combustion)$$

$$= (2.2\%\frac{MJ\ NG\ combusted}{MJ\ throughput})(50.14\frac{gCO_2}{MJ\ NG\ combusted})$$

$$= 1.1031\ gCO_2/MJ \quad \text{(S2)}$$

$$EI_{\text{upstream-dehydration},CO_2} = (Percentage\ of\ NG\ combsuted\ for\ dehydration) \times (Emission\ facotr\ of\ NG\ combustion)$$

$$= (0.12\%\frac{MJ\ NG\ combusted}{MJ\ throughput})(50.14\frac{gCO_2}{MJ\ NG\ combusted})$$

$$= 0.0602\ gCO_2/MJ \quad \text{(S3)}$$

Carbon dioxide emissions from flow back gas flaring: In most cases, the flow back gas is flared. In this study, we use the gas flow back volume obtained from peer-reviewed literature[15] to calculate the carbon dioxide emission. The flare efficiency is assumed to be 98%. The emission intensity is shown:

$$EI_{\text{upstream-flaring},CO_2}$$

$$= \frac{(Flow\ back\ gas\ volume)(Flare\ efficiency)(Heating\ value\ of\ raw\ NG)(Emission\ factor\ of\ NG\ combustion)}{(Gas\ estimated\ ultimate\ recovery)}$$

$$= \frac{\left(0.19\frac{MMscf}{well}\right)(98\%)\left(10^6\frac{scf}{MMscf}\right)\left(1023.1\frac{Btu}{scf}\right)\left(0.00105\frac{MJ}{Btu}\right)\left(50.14\frac{gCO_2}{MJ}\right)}{\left(5.12\frac{Bcf}{well}\right)\left(10^9\frac{scf}{Bcf}\right)\left(1023.1\frac{Btu}{scf}\right)\left(0.00105\frac{MJ}{Btu}\right)}$$

$$= 0.0018\ gCO_2/MJ \quad \text{(S4)}$$

Table S2 summarizes the CO_2 emissions intensity for the upstream stage in the Marcellus basin.

Table S2. Carbon dioxide emission intensity for the upstream stage in the Marcellus basin

CO_2 emission category	**Emission description**	**Raw data**	**Unit**	**Emission intensity (gCO_2/MJ)**
Fuel use	Diesel use for drilling, HF, and wastewater disposal	(Shown in Table S1)	(Shown in Table S1)	0.2836
	NG use for compression	2.2%	MJ of NG combusted/ MJ of NG throughput	1.1031
	NG use for dehydration	0.12%	MJ of NG combusted/ MJ of NG throughput	0.0602
Flaring	Flowback gas flaring	0.19	MMscf/well	0.0018

Methane

Methane emission sources can be divided into several categories: exhaust emission, acid gas removal emissions, flaring, fugitives, venting, and measurement-informed methane emissions.

Methane emissions from exhaust: The exhaust emission factor is obtained from NETL report in the unit of kg CH_4/Mcf NG combusted[4].

The methane emission intensity of exhaust emission during compression and dehydration processes is given by:

$$EI_{\text{upstream-exhaust emission},CH_4} = (Percentage\ of\ NG\ combusted)(Exhaust\ emission\ factor)$$

$$= ((2.2\% + 0.12\%)\frac{MJ\ NG\ combusted}{MJ\ throughput})(947.81\frac{Btu}{MJ})(\frac{1}{1023.1}\frac{scf}{Btu})(10^{-3}\frac{Mcf}{scf})(0.63\frac{kgCH_4}{Mcf\ NG\ combusted})(36000\frac{gCO_2e}{kgCH_4})$$

$$= 0.4875\ gCO_2e/MJ \quad \text{(S5)}$$

Methane emissions from flow back gas flaring: In our study, the flow back gas flaring efficiency is assumed to be 98%, following standard EPA practices. Since the main component in natural gas is methane, the methane emission intensity of flow back gas flaring is calculated, which is given by:

$$\mathrm{EI}_{\text{upstream-flaring},CH_4}$$

$$= \frac{(Flow\ back\ gas\ volume)(1 - Flaring\ efficiency)(Methane\ mole\ fraction\ in\ NG)}{(Gas\ estimated\ ultimate\ recovery)}$$

$$= \frac{\left(0.19\frac{MMscf}{well}\right)(1-98\%)(98.29\%)\left(28328.61\frac{m^3}{MMscf}\right)\left(0.657\frac{kg}{m^3}\right)\left(1000\frac{gCH_4}{kg}\right)\left(36\frac{gCO_2e}{gCH_4}\right)}{\left(5.12\frac{Bcf}{well}\right)\left(10^9\frac{scf}{Bcf}\right)\left(1023.1\frac{Btu}{scf}\right)\left(0.00105\frac{MJ}{Btu}\right)}$$

$$= 0.0005\ gCO_2e/MJ \quad \text{(S6)}$$

Methane emissions from leaks and vents: Methane emission from upstream equipment leaks, pneumatic controllers at the wellhead, and chemical injection pumps are derived from measurements data[5] . In a peer-reviewed bottom-up measurement study in the Appalachian region, no operating chemical injection pumps were encountered at active production sites, either because some chemical injection pumps were solar-powered or had pneumatic injection pumps that had been installed but were not in operation. Therefore, we assume emissions from chemical injection pumps are negligible. The emission intensity of equipment leaks from the upstream facility and pneumatic controllers at the wellhead is given by:

$$\mathrm{EI}_{\text{upstream-equipment leaks},CH_4}$$

$$= \frac{\left(Fugitive\ emission\ rate\ in\ the\ unit\ \frac{scf\ CH_4}{min\cdot well}\right)(well\ lifetime)(Density\ of\ methane)}{(Gas\ estimated\ ultimate\ recovery)}$$

$$= \frac{\left(0.098\frac{scf}{min\cdot well}\right)(32.5years)\left(365\times 24\times 60\frac{mins}{years}\right)\left(\frac{1}{35.3}\frac{m^3}{scf}\right)\left(0.657\frac{kg}{m^3}\right)\left(1000\frac{g}{kg}\right)\left(36\frac{gCO_2e}{gCH_4}\right)}{\left(5.12\frac{Bcf}{well}\right)\left(10^9\frac{scf}{Bcf}\right)\left(1023.1\frac{Btu}{scf}\right)\left(0.00105\frac{MJ}{Btu}\right)}$$

$$= 0.2030\ gCO_2e/MJ \quad \text{(S7)}$$

$$\mathrm{EI}_{\text{upstream-pneumatic wellhead},CH_4}$$

$$= \frac{\left(Fugitive\ emission\ rate\ in\ the\ unit\ \frac{scf\ CH_4}{min\cdot device}\right)(Number\ of\ the\ device)(well\ lifetime)(Density\ of\ methane)}{(Gas\ estimated\ ultimate\ recovery)}$$

$$= \frac{\left(0.126\frac{scf}{min\cdot device}\right)(1\ device)(32.5years)\left(365\times 24\times 60\frac{mins}{years}\right)\left(\frac{1}{35.3}\frac{m^3}{scf}\right)\left(0.657\frac{kg}{m^3}\right)\left(1000\frac{g}{kg}\right)\left(36\frac{gCO_2e}{gCH_4}\right)}{\left(5.12\frac{Bcf}{well}\right)\left(10^9\frac{scf}{Bcf}\right)\left(1023.1\frac{Btu}{scf}\right)\left(0.00105\frac{MJ}{Btu}\right)}$$

$$= 0.2609\ gCO_2e/MJ \quad \text{(S8)}$$

The data for calculation of the emission intensities of pneumatic controllers at the G&B stage and dehydrating venting are obtained from NETL report[4]. In this report, the numbers of high, medium, and low-emissions pneumatic devices are given, and the emission factor of each type of pneumatic device is obtained from the EPA[16]. The emission intensity of pneumatic controllers at the G&B stage is given by:

$$\mathrm{EI}_{\text{upstream-pneumatic G\&B},CH_4} = \frac{(\sum(Number\ of\ each\ device)(Emission\ factor\ of\ each\ device))(Mole\ fraction\ of\ methane)(Density\ of\ methane)}{(Natural\ gas\ throughput)}$$

$$= \frac{\left(29.8 \times 622\frac{scf}{device \cdot day} + 515 \times 218\frac{scf}{device \cdot day} + 68 \times 23\frac{scf}{device \cdot day}\right)\left(365\frac{day}{year}\right)(98.29\%)\left(\frac{1}{35.1}\frac{m^3}{scf}\right)\left(0.657\frac{kg}{m^3}\right)\left(1000\frac{g}{kg}\right)\left(36\frac{gCO_2e}{gCH_4}\right)}{\left(9.13 \times 10^8\frac{Mcf}{year}\right)\left(1000\frac{scf}{Mcf}\right)\left(1023.1\frac{Btu}{scf}\right)\left(0.00105\frac{MJ}{Btu}\right)}$$

$$= 0.0323\ gCO_2e/MJ \quad \text{(S9)}$$

The annual dehydrating venting at the G&B stage is given in the NETL report[4], and the calculation equation is shown:

$$\mathrm{EI}_{\text{upstream-dehydrating venting},CH_4} = \frac{(Annual\ dehydrating\ venting\ emissions)}{(Natural\ gas\ throughput)}$$

$$= \frac{\left(1689\frac{tonnes\ CH4}{year}\right)\left(10^6\frac{g}{tonne}\right)\left(36\frac{gCO_2e}{gCH_4}\right)}{\left(9.13 \times 10^8\frac{Mcf}{year}\right)\left(1000\frac{scf}{Mcf}\right)\left(1023.1\frac{Btu}{scf}\right)\left(0.00105\frac{MJ}{Btu}\right)}$$

$$= 0.0617\ gCO_2e/MJ \quad \text{(S10)}$$

Methane emissions from other sources: For methane emission from acid gas removal, flaring at G&B, gathering pipelines, and blowdowns, we directly use the emission intensities from the life cycle analysis of Appalachian natural gas in NETL report since specific emission data are not available. The obtained emission intensities from NETL report are in unit of g CO_2/MJ LNG delivered, which are normalized to g CO_2e/MJ stage throughput by multiplying the ratio of natural gas at production and delivered gas. The ratio of natural gas at production and delivered gas are calculated based on the gas energy flow of East Texas basin as an approximation. [3,12]

Measurement informed methane emissions: Analysis of recent field measurements across oil and gas production facilities in the US shows that measured emissions are higher than official inventory estimates. To address this issue in lifecycle assessment, we introduce measurement into our analysis. For easy comparison between inventory estimates and measurements estimates, we calculate the inventory-based natural gas emission rate by aggregating all bottom-up process-level methane emission intensities and converting from the unit of gCO_2e/MJ throughput to MJ NG emitted/MJ throughput, which is shown:

$$ER_{\text{upstream-inventory}} = \frac{(\sum Methane\ emission\ factor)(Higher\ heating\ value\ of\ raw\ natural\ gas)}{(Density\ of\ methane)(Mole\ fraction\ of\ CH_4)}$$

$$= \frac{\left(1.2700\frac{gCO_2e}{MJ}\right)\left(\frac{1}{36}\frac{gCH_4}{gCO_2e}\right)\left(\frac{1}{1000}\frac{kg\ CH_4}{gCH_4}\right)\left(1023.1\frac{Btu}{scf\ NG}\right)\left(0.001055\frac{MJ}{Btu}\right)}{\left(0.657\frac{kgCH_4}{m^3CH_4}\right)\left(\frac{1}{35.3}\frac{m^3CH_4}{scfCH_4}\right)\left(98.29\%\frac{scfCH_4}{scfNG}\right)}$$

$$= 0.21\%\ \frac{MJ\ NG\ emitted}{MJ\ throughput} \quad \text{(S11)}$$

The measured natural gas emission rate in the northeastern Marcellus basin is 0.40%, which is obtained from a measurement campaign over this region.[6] Since the measured emission rate is normalized to gross gas production, we normalize it to stage throughput by multiplying the energy content fraction of dry gas at upstream. Finally, the energy normalized methane emission rate from the upstream stage in the northeastern Marcellus basin is estimated to be 0.39% (MJ NG emitted/MJ throughput).

The top-down measured natural gas emission rate includes all emissions in the production and G&B stage, so it cannot be directly added to lifecycle inventory without first addressing overlap with bottom-up calculation methods. In order to avoiding double counting, we subtract inventory-based from measurement-informed emission rate and use the remainder to represent the portion of the emissions that were missed by inventory estimates, shown as:

$$EI_{\text{upstream-diff btw meas \& inventory, } CH_4}$$

$$= \frac{(Difference\ between\ measured\ and\ inventory\ emission\ rate)(Mole\ fraction\ of\ CH_4)(Density\ of\ methane)}{(Heating\ value\ of\ NG)}$$

$$= \frac{\left((0.39\% - 0.21\%)\frac{MJ\ of\ NG\ emitted}{MJ}\right)\left(947.82\frac{Btu}{MJ}\right)\left(98.29\%\frac{scfCH_4}{scfNG}\right)\left(\frac{1}{35.3}\frac{m^3}{scf}\right)\left(0.657\frac{kgCH4}{m^3CH4}\right)\left(1000\frac{g}{kg}\right)\left(36\frac{gCO_2e}{gCH_4}\right)}{\left(1023.1\frac{Btu}{scf}\right)}$$

$$= 1.1094\ gCO_2e/MJ \quad \text{(S12)}$$

Table S3 summarize methane emissions intensities at the upstream stage for the Marcellus basin lifecycle assessment.

Table S3. Methane emission intensities at the upstream stage in the Marcellus basin

Methane emission category	**Emission description**	**Raw data**	**Unit**	**Emission intensity (gCO_2e/MJ)**
Fuel use		2.32%	MJ of NG combusted /MJ throughput	0.4875

	Exhaust emission from compression and other operation		0.63	kgCH_4/Mcf NG combusted	
Acid gas removal	Acid gas removal		0.0293	gCO_2e/MJ	0.0293
Flaring	Flow back gas flaring		0.19	MMscf flowback gas/well	0.0005
	Flow stacks at G&B		0.0065	gCO_2e/MJ	0.0065
Fugitives	Equipment leaks from the upstream facility		0.098	scf CH_4/min/well	0.2030
	Gathering pipelines		0.0231	gCO_2e/MJ	0.0231
Venting	Pneumatic controllers at the wellhead		0.126	scf CH_4/min/device	0.2609
	Liquid unloading		0.03%	hr venting/hr production	0.1525
	Chemical injection pumps		/	/	0
	Blowdowns		0.0359	gCO_2e/MJ	0.0359
	Pneumatic controllers in G&B	Number of high bleed device	29.8	devices	0.0323
		Number of intermittent bleed device	515		
		Number of intermittent bleed device	68		
		EF of high bleed device	622	scf/device-day	
		EF of high bleed device	218		
		EF of high bleed device	23		
	Dehydrator venting in G&B		1689	tonnes CH4/facility-year	0.0617
Difference between measurement-informed and inventory-based emission intensity	Inventory based emission rate		0.21%	MJ of NG emitted/MJ throughput	1.1094
	Energy normalized measurement informed emission rate		0.39%		

S 2.2 Permian basin

Carbon dioxide

Table S4 shows all carbon dioxide emission intensities in the Permian basin. The carbon dioxide emission intensity for diesel used for drilling, HF, and wastewater disposal in the Permian basin is similar to that in the Marcellus basin, the only difference is that the denominator is the total energy content of both produced gas, crude oil and lease condensate. In our study, the estimated ultimate recovery of Permian basin natural gas and crude oil are 1.36×10^7 Mcf and 1.67×10^6 bbl[3]. The heating value of crude oil is 5.6

MMBtu/bbl obtained from Rosselot et al. study.[12] The heating value of produced natural gas is 1225 Btu/scf, which is calculated based on composition data obtained from Contreras et al. study.[17] The emission intensities for NG use for compression, NG use for dehydration, acid gas removal, and flare stacks at production are all obtained from the NETL report[3]. The obtained emission intensities from NETL report are in unit of g CO_2/MJ LNG delivered, which are normalized to g CO_2e/MJ stage throughput by multiplying the ratio of natural gas at production and delivered gas. The ratio of natural gas at production and delivered gas are calculated based on the gas energy flow of Permian basin.[12]

Table S4. Carbon dioxide emission intensities at the upstream stage in the Permian basin

CO_2 emission category	**Emission description**	**Emission intensity (gCO_2/MJ throughput)**
Fuel use	Diesel use for drilling, HF, and wastewater disposal	0.0570
	NG use for compression	1.8863
	NG use for dehydration	0.3983
Acid gas removal	Acid gas removal	0.0121
Flaring	Flaring stacks at production	0.0602

Methane

The emission intensities for all inventory based processes are obtained from NETL report[3]. The obtained emission intensities from NETL report are in unit of g CO_2/MJ LNG delivered, which are normalized to g CO_2e/MJ stage throughput by multiplying the ratio of natural gas at production and delivered gas. The ratio of natural gas at production and delivered gas are calculated based on the gas energy flow of Permian basin.[12]

The measured natural gas emission rate in the Permian basin is 3.52%, which is a satellite-based emission rate over entire Permian basin.[8] Since the measured emission rate is normalized to gross gas production, we normalize it to stage throughput by multiplying the energy content fraction of dry gas at the upstream stage. Finally, the measured informed gas emission rate from the upstream stage in the Permian basin is 1.10% (MJ NG emitted/MJ throughput). The difference between measurement-informed and inventory-based emission intensity calculation process is the same as that in the Marcellus basin.

Table S5. Methane emission intensities at the upstream stage in the Permian basin

CH_4 emission category	Emission description	Emission intensity (gCO_2e/MJ throughput)
Fuel use	Exhaust emission from compression and other operations	0.9844
Acid gas removal	Acid gas removal	0.0282
Flaring	Flare stacks at production	0.0136
	Flare stacks at G&B	0.0055
Fugitives	Equipment leaks from the production facility	0.0447
	Gathering pipelines	0.0156
Venting	Pneumatic controllers at the wellhead	0.6004
	Liquids unloading	0.0466
	Pneumatic pumps	0.0078
	Blowdowns	0.0070
	Pneumatic controllers in G&B	0
	Dehydrator venting in G&B	0
Difference between measurement-informed and inventory-based emission intensity	Emission difference between inventory estimates and top-down measurements	3.1530

S 3. Processing stage emission inventory

The processing plant is primarily powered by the combustion of fuel gas and electricity from the local grid. The facility fuel gas consumption rate and compressor power requirement in the Marcellus basin are extracted from ExxonMobil operation data in peer-reviewed literature[2], whereas, for the Permian basin, all energy requirement data comes from GHGRP[18,19], which represents the US average data from 2018. Like the upstream process, the methane emission during the processing stage also mainly comes from flares, equipment leaks, acid gas removal unit, and some intentional or controlled venting processes.

S 3.1 Marcellus basin

Carbon Dioxide

In general, the carbon dioxide emission from the processing stage comes from fuel gas combustion, power use, acid gas removal, and flare stacks.

Carbon dioxide emissions from fuel gas combustion: We estimated the CO_2 emissions of fuel gas combustion and power use associated with the processing stage based on the energy consumption and natural gas heating value data available in the peer-reviewed literature[2]. Due to the high electrification degree in the Marcellus basin, the gas consumption is only 0.25 MMscf/day. The heating value of the produced natural gas from the Marcellus basin is 1023.1 Btu/scf. The carbon dioxide emissions coefficient of natural gas combustion is 116.65 lb CO_2/MMBtu of natural gas, which is obtained from the Energy

Information Administration[20]. The amount of gas entering the processing plant is 131.52 MMscf/day. The CO_2 emission intensity for the gas combustion in the processing plant is given by:

$$\mathrm{EI}_{\text{proc-gas combustion},CO_2} = \frac{(Gas\ consumption)(Emission\ facotr)}{(Natural\ gas\ entered)}$$

$$= \frac{\left(0.25\frac{MMscf}{day}\right)\left(1023.1\frac{Btu}{scf}\right)\left(116.65\frac{lb}{MMBtu}\right)\left(453.51\frac{g}{lb}\right)}{\left(131.52\frac{MMscf}{day}\right)\left(1023.1\frac{Btu}{scf}\right)\left(1055.056\frac{MJ}{MMBtu}\right)}$$

$$= 0.0953\ gCO_2/MJ \quad \text{(S13)}$$

Carbon dioxide emissions from power use: The estimation of the emission from power use follows a similar process. The power consumption of the processing facility in the Marcellus basin is 51.52 hp/(MMscf/day throughput). The gas throughput of this processing plant is 119.03 MMscf/day, which equals the amount of gas exiting the processing plant. The carbon dioxide emission coefficient of power is 1.037 lb CO_2/kWh[21]. The CO_2 emission intensity of the power use in the processing plant is given by:

$$\mathrm{EI}_{\text{proc-power use},CO_2} = \frac{(Power\ use)(Emission\ facotr)}{(Natural\ gas\ entered)}$$

$$= \frac{\left(51.52\frac{hp}{\frac{MMscf}{day}} \times 24hr\right)\left(119.03\frac{MMscf}{day}\right)\left(1.037\frac{lb}{kWh}\right)\left(0.7457\frac{kWh}{hph}\right)\left(453.51\frac{g}{lb}\right)}{\left(131.52\frac{MMscf}{day}\right)\left(1023.1\frac{Btu}{scf}\right)\left(1055.056\frac{MJ}{MMBtu}\right)}$$

$$= 0.3636\ gCO_2/MJ \quad \text{(S14)}$$

Carbon dioxide emissions from acid gas removal: Apart from the specific energy consumption data, other emissions data of the processing plant are not available for the Marcellus basin, so we use the 2018 US average profile[18,19] to supplement. During the acid gas removal process, the total CO_2 emission is 24600 tonnes/year[22]. The heating value of produced natural gas is 1.235 MMBtu/Mcf. The annual produced natural gas entering the processing plant is 3.69×10^7 Mcf. The CO_2 emission intensity of the acid gas removal is shown:

$$\mathrm{EI}_{\text{proc-acid gas removal},CO_2} = \frac{(Annual\ mass\ emission)}{(Natural\ gas\ entered)}$$

$$= \frac{(24600\ tonnes)\left(10^6\frac{g}{tonnes}\right)}{(3.69 \times 10^7 Mcf)\left(1.235\frac{MMBtu}{Mcf}\right)\left(1055.056\frac{MJ}{MMBtu}\right)}$$

$$= 0.5114\ gCO_2/MJ \quad \text{(S15)}$$

Carbon dioxide emissions from flaring: The annual natural gas flared in the processing plant is 1.74×10^8scf. We assume the flaring efficiency is 98%. The CO_2 emission intensity of the flaring in the processing plant is given by:

$$EI_{\text{proc-flaring},CO_2} = \frac{(Annual\ gas\ flared)(Flaring\ efficiency)(Emission\ facotr\ of\ gas\ combustion)}{(Natural\ gas\ entered)}$$

$$= \frac{(1.74\times10^8 scf)(98\%)\left(1.235\frac{MMBtu}{Mcf}\right)\left(\frac{1}{1000}\frac{Mcf}{scf}\right)\left(116.65\frac{lb}{MMBtu}\right)\left(453.51\frac{g}{lb}\right)}{(3.69\times10^7 Mcf)\left(1.235\frac{MMBtu}{Mcf}\right)\left(1055.056\frac{MJ}{MMBtu}\right)}$$

$$= 0.2316\ gCO_2/MJ \quad \text{(S16)}$$

The carbon dioxide emission intensity at processing stage for Marcellus basin is summarized in Table S6.

Table S6. Carbon dioxide emission intensities for the processing stage in the Marcellus basin

Carbon dioxide emission category	**Emission description**	**Emission intensity (gCO_2/MJ)**
Energy use	Fuel gas combustion	0.0953
	Power use	0.3636
Acid gas removal	Acid gas removal	0.5114
Flaring	Flare stacks	0.2316

Methane

Methane emissions from exhaust: The exhaust emission intensity of turbine and efficiency of the turbine is obtained from Zimmerle et al.[23] . The methane emission intensity of exhaust emission from centrifugal compressors is given by:

$$EI_{\text{proc-exhaust emission},CH_4} = \frac{(Gas\ consumption)(Turbne\ thermal\ efficiency)(Exhaust\ emission\ facotr)}{(Natural\ gas\ entered)}$$

$$= \frac{\left(0.25\frac{MMscf}{day}\right)\left(1023.1\frac{Btu}{scf}\right)(33.6\%)\left(0.031\frac{gCH_4}{hp\cdot hr}\right)\left(36\frac{gCO_2e}{gCH_4}\right)\left(10^6\frac{scf}{MMscf}\right)\left(0.000393\frac{hp\cdot hr}{Btu}\right)}{\left(131.52\frac{MMscf}{day}\right)\left(1023.1\frac{Btu}{scf}\right)\left(1055.056\frac{MJ}{MMBtu}\right)}$$

$$= 0.0003\ gCO_2e/MJ \quad \text{(S17)}$$

Methane emissions from acid gas removal: The methane emission intensity of acid gas removal is given by:

$$\mathrm{EI}_{\text{proc-acid gas removal},CH_4} = \frac{(Methane\ emission\ from\ acid\ gas\ removal\ unit)}{(Natural\ gas\ entered)}$$

$$= \left(3.73 \times 10^{-5}\ \frac{kgCH_4}{kg\ NG}\right)\left(1000\frac{gCH_4}{kgCH_4}\right)\left(36\frac{gCO_2e}{gCH_4}\right)\left(0.66\frac{kg\ NG}{m^3}\right)\left(28.33\frac{m^3}{Mcf}\right)\left(\frac{1}{1.235}\frac{Mcf}{MMBtu}\right)\left(9.48 \times 10^{-4}\frac{MMBtu}{MJ}\right)$$

$$= 0.0195\ gCO_2e/MJ \quad \text{(S18)}$$

Methane emissions from flaring: The methane emission intensity of flaring is given by:

$$\mathrm{EI}_{\text{proc-flaring},CH_4} = \frac{(Annual\ gas\ flared)(1 - Flaring\ efficiency)(CH4\ mass\ fraction)}{(Natural\ gas\ entered)}$$

$$= \frac{(1.74 \times 10^8 scf)(1 - 98\%)\left(0.66\frac{kg}{m^3}\right)\left(\frac{1}{35.3}\frac{m^3}{scf}\right)\left(0.862\frac{kgCH_4}{kgNG}\right)\left(1000\frac{g}{kg}\right)\left(36\frac{gCO_2e}{gCH_4}\right)}{(3.69 \times 10^7 Mcf)\left(1.235\frac{MMBtu}{Mcf}\right)\left(1055.056\frac{MJ}{MMBtu}\right)}$$

$$= 0.0424\ gCO_2e/MJ \quad \text{(S19)}$$

Methane emissions from leaks and vents: The methane emission intensity of fugitives, venting (except high bleed pneumatic devices) is given by:

$$\mathrm{EI}_{\text{proc-xx},CH_4} = \frac{(Annual\ mass\ emission)}{(Natural\ gas\ entered)}$$

$$= \frac{(\ Annual\ emissions\ in\ tonnes)\left(10^6\frac{g}{tonnes}\right)\left(36\frac{gCO_2e}{gCH_4}\right)}{(3.69\times10^7 Mcf)\left(1.235\frac{MMBtu}{scf}\right)\left(1055.056\frac{MJ}{MMBtu}\right)} \quad \text{(S20)}$$

The emission intensity of high bleed pneumatic devices is obtained from Environmental Protection Agency[16]. The methane emission intensity of high-bleed pneumatic devices is given by:

$$\mathrm{EI}_{\text{proc-high bleed},CH_4}$$

$$= \frac{(Emission\ factor\ of\ high\ bleed\ pneumatic\ devices)(Operating\ time)(Count)(CH4\ mass\ fraction)}{(Natural\ gas\ entered)}$$

$$= \frac{\left(622\frac{scf}{devices \cdot day}\right)(3170hrs)(1devices)\left(\frac{1}{24}\frac{day}{hrs}\right)\left(0.66\frac{kg\ NG}{m^3}\right)\left(\frac{1}{35.3}\frac{m^3}{scf}\right)\left(0.862\frac{kg\ CH_4}{kg\ NG}\right)\left(10^6\frac{g}{tonnes}\right)\left(36\frac{gCO_2e}{gCH_4}\right)}{(3.69 \times 10^7 Mcf)\left(1.235\frac{MMBtu}{scf}\right)\left(1000\frac{scf}{Mcf}\right)\left(1055.056\frac{MJ}{MMBtu}\right)}$$

$$= 0.0010\ gCO_2e/MJ \quad \text{(S21)}$$

Measurement informed methane emissions: Since there is no specific processing plant measurements in northeastern Marcellus basin, we use lower bound of measured emission rate in processing plant in southwestern Marcellus basin for approximation, which is 0.137% normalized to gross dry gas production[24]. Then the gross dry gas production normalized measured emission rate is converted to normalized to stage throughput by multiplying the fraction of dry gas to total stage throughput. The energy normalized measured methane emission rate in processing plant is 0.133% (MJ NG emitted/MJ of the produced gas entering the processing plant).

The inventory-based natural gas emission rate is given by:

$$\mathrm{ER}_{\text{proc-inventory}} = \frac{(\sum Methane\ emission\ factor)(Heating\ value\ of\ raw\ natural\ gas)}{(Density\ of\ methane)(Mole\ fraction\ of\ CH4)}$$

$$= \frac{\left(0.1387\frac{gCO2e}{MJ}\right)\left(\frac{1}{36}\frac{gCH_4}{gCO2e}\right)\left(\frac{1}{1000}\frac{kgCH_4}{gCH_4}\right)\left(1023.1\frac{Btu}{scf\ NG}\right)\left(0.001055\frac{MJ}{Btu}\right)}{\left(0.657\frac{kgCH_4}{m^3CH_4}\right)\left(\frac{1}{35.3}\frac{m^3CH_4}{scfCH_4}\right)\left(98.29\%\frac{scfCH_4}{scfNG}\right)}$$

$$= 0.023\%\ \frac{MJ\ NG\ emitted}{MJ\ produced\ gas\ entering\ into\ processing} \qquad \text{(S22)}$$

After obtaining the inventory-based emission rate and measurements-informed emission rate, we calculate the difference between measurement-informed and inventory based emission intensity in the processing plant is given by:

$$\mathrm{EI}_{\text{proc-diff btw meas \& inventory, } CH_4}$$

$$= \frac{(Difference\ between\ measured\ and\ inventory\ emission\ rate)(Mole\ fraction\ of\ CH_4)(Density\ of\ methane)}{(Heating\ value\ of\ NG)}$$

$$= \frac{\left((0.133\% - 0.023\%)\frac{MJ\ of\ NG\ emitted}{MJ}\right)\left(947.82\frac{Btu}{MJ}\right)\left(98.29\%\frac{scfCH_4}{scfNG}\right)\left(\frac{1}{35.3}\frac{m^3}{scf}\right)\left(0.657\frac{kgCH_4}{m^3CH_4}\right)\left(1000\frac{g}{kg}\right)\left(36\frac{gCO_2e}{gCH_4}\right)}{\left(1023.1\frac{Btu}{scf}\right)}$$

$$= 0.6746\ gCO_2e/MJ \qquad \text{(S23)}$$

Table S7. Methane emission intensities of processing stage in Marcellus basin

Methane emission category	**Emission description**	**Raw data**	**Unit**	**Emission intensity (gCO_2e/MJ)**
Energy use	Exhaust emission from centrifugal compressors	0.031	gCH_4/hp-hr	0.0003
Acid gas removal	Acid gas removal	3.73×10^{-5}	kg CH_4/kg NG	0.0195
Flaring	Flare stacks	1.74×10^{8}	scf	0.0424

Fugitives	Equipment leaks		19.4	tonnes/year	0.0145
Venting	High-bleed pneumatic devices	Operating hour	3170	hrs	0.0010
		Count	1	/	
		Emission factor	622	scf/device-day	
	Dehydrators		16.49	tonnes/year	0.0123
	Compressor venting		15.40	tonnes/year	0.0115
	Emergency shutdown venting		5.45	tonnes/year	0.0041
	Facility piping venting		38.7	tonnes/year	0.0290
	Pigging venting		1.81	tonnes/year	0.0014
	Scrubber venting		0.423	tonnes/year	0.0003
	Other sources		3.41	tonnes/year	0.0026
Difference between measurement-informed and inventory-based emission intensity	Inventory based emission rate		0.023%	MJ of NG emitted/MJ of produced gas entering in processing	0.6746
	Measurement informed emission rate		0.133%		

S 3.2 Permian basin

For the Permian basin, since there is no specific emission intensity for the processing plant, we use the US average profile in 2018 to estimate the emission inventory[18,19]. Then, the measurement-informed emissions are calculated to better characterize the greenhouse gas emissions in the Permian basin. The calculating procedure for these emission intensities is similar to that in the Marcellus basin.

Carbon dioxide

The carbon dioxide emission intensities at the processing stage in the Permian basin are shown in Table S8.

Table S8. Carbon dioxide emission intensities for the processing stage in the Permian basin

Carbon dioxide emission category	**Emission description**		**Raw data**	**Unit**	**Emission intensity (gCO_2/MJ)**
Energy use	Fuel gas combustion	Centrifugal	5.45×10^7	hp-hr	1.2761
		Reciprocating	9.24×10^7		
	Power use		0	/	0
Acid gas removal	Acid gas removal		24600	tonnes/year	0.5114
Flaring	Flare stacks		1.74×10^8	scf	0.2316

Methane

The measured methane emission rate from processing plant in the Permian basin is 0.185%, which is obtained from a measurement campaigns over the whole Permian basin.[8] Since the measured emission rate

is calculated based on the gross dry gas production, we convert it to produced gas based methane emission rate. Finally, the energy normalized measured methane emission rate from the processing plant in the Permian basin is 0.138% (MJ NG emitted/MJ of the produced gas entering the processing plant). The inventory emission rate is 0.045%, which is calculated in the same way as in the Marcellus basin. Table S9 show the methane emission intensities for the processing plant in the Permian basin.

Table S9. Methane emission intensities for the processing stage in the Permian basin

Methane emission category	**Emission description**		**Raw data**	**Emission intensity (gCO_2e/MJ)**
Energy use	Exhaust emission from centrifugal compressors		46	0.0344
	Exhaust emission from reciprocating compressors		97.3	0.0728
Acid gas removal	Acid gas removal		3.73×10^{-5}	0.0255
Flaring	Flare stacks		1.74×10^{8}	0.0555
Fugitives	Equipment leaks		19.4	0.0145
Venting	High-bleed pneumatic devices	Operating hour	3170	0.0013
		Count	1	
		Emission factor	622	
	Dehydrators		16.49	0.0123
	Compressor venting		15.40	0.0115
	Emergency shutdown venting		5.45	0.0041
	Facility piping venting		38.7	0.0290
	Pigging venting		1.81	0.0014
	Scrubber venting		0.423	0.0003
	Other sources		3.41	0.0026
Difference between measurement-informed and inventory-based emission intensity	Inventory based emission rate		0.045%	0.5456
	Measurement informed emission rate		0.141%	

S 4. Transmission stage emission inventory

Since the Gulf Coast liquefaction facilities account for more than 90% of the US total liquefaction capacity, it was assumed that the gas exiting from the processing plant in both Marcellus and Permian basins is transported to the Sabine Pass liquefaction facility . The driving distance on Google Maps was used to approximate the pipeline length between processing plant and liquefaction facility. It is assumed that the Marcellus gas is sent 1294 miles away from the processing plant to the Sabine Pass liquefaction facility, however, in the Permian basin LNG supply chain, the distance between the processing plant and the Sabine

Pass liquefaction facility is 600 miles. Given the distance between the processing plant and liquefaction facility, the distance between two adjacent transmission stations, and the US average percentage of each type of compressor, we calculated the number of each type of compressor station required in each LNG supply chain. Combining the horsepower, operating time, and thermal efficiency of each compressor station, we finally get the amount of natural gas that is needed to power the transmission system. Multiplied by the carbon dioxide coefficient and exhaust emission intensity respectively, the carbon dioxide emissions from the fuel use in the transmission stage are quantified.

In addition to the emissions from burning natural gas, fugitive and venting emissions are also significant in the transmission stage. The emission rates of all fugitive and venting items of each type of compressor station come from Zimmerle et al. study[23], which is based on 2292 onsite measurements in the transmission and storage sector across the US.

S 4.1 Marcellus basin

Carbon dioxide

During the transmission stage, the carbon dioxide emission mainly comes from the fuel use in compression station. The distance between two adjacent compressor stations is 55 miles.[25] Therefore, there are 24 compressor stations along the transmission line from the Marcellus basin processing plant to the Sabine Pass liquefaction facility. The number of each type of compressor station is calculated based on the percentage of each kind of compressor station obtained from Zimmerle et al. work, which represents the US average composition. The operating hour, house power, thermal efficiency, and other parameters are shown in Table S10.

Table S10. Parameters for emission intensities of fuel use during the transmission stage

Parameter	Value	Data source
Percentage of reciprocating engine-powered compressor station	77%	Zimmerle et al. (2015)[23]
Percentage of centrifugal turbine powered compressor station	23%	
Number of reciprocating engine powered compressor station	18	Based on calculation
Number of centrifugal turbine powered compressor station	6	Based on calculation
Horsepower of reciprocating engine powered compressor station (hp)	10942	Zimmerle, et al. (2015)[23]
Horsepower of centrifugal turbine powered compressor station (hp)	18988	
Operating hours of reciprocating compressor stations (hr/year)	2890	
Operating hours of centrifugal compressor stations (hr/year)	2587	

Thermal efficiency of reciprocating engines	44%	NETL report [3]
Thermal efficiency of turbines	26%	
Natural gas throughput (Mcf/facility-year)	1.24E+08	NETL report [4]
Heating value of dry gas(Btu/scf)	1036	EIA[26]
Emission intensity of NG combustion (gCO_2/MJ)	50.14	EIA [20]

The emission intensity of carbon dioxide during the transmission stage is given by:

$$EI_{\text{tran-fuel use, } CO_2} = \frac{\left(\sum \frac{(Number\ of\ compressor\ station)(Operating\ hour)(housepower)}{Thermal\ efficiency}\right)(EF\ of\ NG\ combustion)}{(Natural\ gas\ throughput)}$$

$$= \frac{\left(\frac{18 * 10942\ hp * 2890\ hr}{44\%} + \frac{6 * 18988\ hp * 2587\ hr}{26\%}\right)\left(0.7457\frac{kWh}{hph}\right)\left(3.6\frac{MJ}{kWh}\right)\left(50.14\frac{gCO_2}{MJ}\right)}{\left(1.24 \times 10^8\frac{mcf}{facility \cdot year}\right)\left(1000\frac{scf}{mcf}\right)\left(1036\frac{Btu}{scf}\right)\left(0.001055\frac{MJ}{Btu}\right)}$$

$$= 2.4109\ gCO_2/MJ \quad \text{(S24)}$$

Methane

The methane emission during the transmission stage can be divided into three categories: exhaust emission, fugitives, and venting. Fugitive emissions include leaks from both transmission stations and pipelines. The venting emissions include pneumatic devices venting on transmission stations, other transmission station venting, and pipeline venting.

Methane emissions from exhaust: The exhaust emission caused by fuel gas combustion is calculated based on the total energy of natural gas combustion and exhaust emission factor obtained from Zimmerle et al. study[23]. The methane emission intensity of exhaust emission is given by:

$$EI_{\text{tran-exhaust emission, } CH_4} = \frac{\left(\sum \frac{(Number\ of\ compressor\ station)(Operating\ hour)(housepower)(EF\ of\ exhaust\ emission)}{Thermal\ efficiency}\right)}{(Natural\ gas\ throughput)}$$

$$= \frac{\left(\frac{18 * 10942\ hp * 2890\ hr * 3.7\frac{gCH_4}{hp \cdot hr}}{44\%} + \frac{6 * 18988\ hp * 2587\ hr * 0.031\frac{gCH_4}{hp \cdot hr}}{26\%}\right)\left(36\frac{gCO_2e}{gCH_4}\right)}{\left(1.24 \times 10^8\frac{Mcf}{facility \cdot year}\right)\left(1000\frac{scf}{Mcf}\right)\left(1036\frac{Btu}{scf}\right)\left(0.001055\frac{MJ}{Btu}\right)}$$

$$= 1.2810\ gCO_2e/MJ \quad \text{(S25)}$$

Methane emissions from leaks and vents: In this study, we use the transmission measurements data from Zimmerle et al.[23] for calculating fugitive and venting emissions at transmission station of Marcellus basin sourced LNG supply chains. The transmission station emission rate is combined with number and type of transmission station to obtain emission intensities of each category of fugitive and venting emissions. The emission from pipeline fugitives and venting is calculated based on the GHGRP data[18,19,22], representing US 2018 average. The parameters used for calculation and calculated emission intensities for Marcellus basin are shown in Table S11. The equations used for calculation of these emission intensities are shown after Table S11.

Table S11. Fugitive and venting emission intensities at transmission stage for Marcellus basin

Methane emission source	**Parameters**	**Value**	**Data source**	**Emission intensity (gCO_2e/MJ)**
Transmission station fugitives	Station fugitives (Mg CH_4/station)	64	Zimmerle et al. (2015)[23]	2.0757
	Reciprocating compressor fugitives (Mg CH_4/compressor)	64		
	Number of reciprocating compressors	18	Engineering based calculation	
	Centrifugal compressor fugitives (Mg CH_4/compressor)	54.5	Zimmerle et al. (2015)[23]	
	Number of centrifugal compressors	6	Engineering based calculation	
	Uncategorized fugitives (Mg CH_4/station)	200	Zimmerle et al. (2015)[23]	
Pipeline fugitives	Pipeline fugitives (kg CH_4/mile)	1120	GHGRP data[18,19,22]	0.0354
	Transmission distance (mile)	1294		
Pneumatic devices venting	Pneumatic devices venting (Mg CH_4/device)	1	Zimmerle et al. (2015)[23]	0.1020
	Number of pneumatic devices	16	Assumption	
Transmission station venting	Station venting (Mg CH_4/station)	57	Zimmerle et al. (2015)[23]	0.3634
Pipeline venting	Pipeline venting (ton CH_4/year for 10,100 miles pipeline)	3810	GHGRP data[18,19,22]	0.0119
	Transmission distance (mile)	1294		

The calculation equation for the transmission station fugitives is shown below:

$$\mathrm{EI}_{\text{tran-station fugitives, } CH_4}$$

$$= \frac{\big((Station\ and\ uncategorized\ fugitives\ emission\ rate)(Station\ number) + (Compressor\ fugitives\ emission\ rate\ )(compressor\ number)\big)(GWP\ of\ methane)}{(Transmission\ station\ NG\ throughput)}$$

$$= \frac{\left(\left(64\frac{Mg\ CH_4}{station} + 200\frac{Mg\ CH_4}{station}\right)(24\ station) + \left(64\frac{MgCH_4}{compressor} \times 18 + 54.5\frac{MgCH_4}{compressor} \times 6\right)\right)\left(10^6\frac{g\ CH_4}{Mg\ CH_4}\right)\left(36\frac{gCO_2e}{gCH_4}\right)}{\left(1.24 \times 10^8\frac{Mcf}{facility \cdot year}\right)\left(10^3\frac{scf}{Mcf}\right)\left(1036\frac{Btu}{scf\ NG}\right)\left(0.001055\frac{MJ}{Btu}\right)}$$

$$= 2.0757\ gCO_2e/MJ \quad \text{(S26)}$$

The calculation equation for the pipeline fugitives is shown below:

$$\mathrm{EI}_{\text{tran-pipeline fugitives, } CH_4}$$

$$= \frac{(Pipeline\ fugitives\ emission\ rate)(pipeline\ distance)(GWP\ of\ methane)}{(Transmission\ station\ NG\ throughput)}$$

$$= \frac{\left(1120\frac{kg\ CH_4}{mile}\right)(1294\ miles)\left(10^3\frac{g\ CH_4}{kg\ CH_4}\right)\left(36\frac{gCO_2e}{gCH_4}\right)}{\left(1.35 \times 10^9\frac{Mcf}{facility \cdot year}\right)\left(10^3\frac{scf}{Mcf}\right)\left(1036\frac{Btu}{scf\ NG}\right)\left(0.001055\frac{MJ}{Btu}\right)}$$

$$= 0.0354\ gCO_2e/MJ \quad \text{(S27)}$$

The calculation equation for the pneumatic device venting is shown below:

$$\mathrm{EI}_{\text{tran-pneumatic device, } CH_4}$$

$$= \frac{(Pneumatic\ devices\ emission\ rate)(Number\ of\ pneumatic\ device)(Number\ of\ transmission\ station)(GWP\ of\ methane)}{(Transmission\ station\ NG\ throughput)}$$

$$= \frac{\left(1\frac{Mg\ CH_4}{device}\right)\left(16\ \frac{devices}{station}\right)(24\ station)\left(10^6\frac{g\ CH_4}{Mg\ CH_4}\right)\left(36\frac{gCO_2e}{gCH_4}\right)}{\left(1.24 \times 10^8\frac{Mcf}{facility \cdot year}\right)\left(10^3\frac{scf}{Mcf}\right)\left(1036\frac{Btu}{scf\ NG}\right)\left(0.001055\frac{MJ}{Btu}\right)}$$

$$= 0.1020\ gCO_2e/MJ \quad \text{(S28)}$$

The calculation equation for the transmission station venting is given by:

$$\mathrm{EI}_{\text{tran-station venting, } CH_4}$$

$$= \frac{(Transmission\ station\ venting\ rate)(Number\ of\ transmission\ station)(GWP\ of\ methane)}{(Transmission\ station\ NG\ throughput)}$$

$$= \frac{\left(57\frac{Mg\ CH_4}{station}\right)(24\ station)\left(10^6\frac{g\ CH_4}{Mg\ CH_4}\right)\left(36\frac{gCO_2e}{gCH_4}\right)}{\left(1.24 \times 10^8\frac{Mcf}{facility \cdot year}\right)\left(10^3\frac{scf}{Mcf}\right)\left(1036\frac{Btu}{scf\ NG}\right)\left(0.001055\frac{MJ}{Btu}\right)}$$

$$= 0.3634\ gCO_2e/MJ \quad \text{(S29)}$$

The calculation equation for the pipeline venting is shown below:

$$EI_{\text{tran-pipeline venting, } CH_4}$$

$$= \frac{(Pipeline\ venting\ rate)(Pipeline\ distance)(GWP\ of\ methane)}{(Transmission\ station\ NG\ throughput)}$$

$$= \frac{\left(3810\frac{tone\ CH_4}{year}\right)\left(\frac{1294}{10100}\frac{miles}{miles}\right)\left(10^6\frac{g\ CH_4}{Mg\ CH_4}\right)\left(36\frac{gCO_2e}{gCH_4}\right)}{\left(1.35\times10^9\frac{Mcf}{facility\cdot year}\right)\left(10^3\frac{scf}{Mcf}\right)\left(1036\frac{Btu}{scf\ NG}\right)\left(0.001055\frac{MJ}{Btu}\right)}$$

$$= 0.0119\ gCO_2e/MJ \quad \text{(S30)}$$

S 4.2 Permian basin

Carbon dioxide

For the Permian basin, the distance between the processing plant and the Sabine Pass liquefaction facility is 600 miles. Therefore, given the distance between two adjacent stations is 55 miles, there are 11 compressor stations along the natural gas transmission line, 8 of each are reciprocating engine powered compressor stations and 3 of which are centrifugal turbine powered compressor stations. Other parameters are the same as in the Marcellus basin and are not shown again here. Following the same calculation process as in the Marcellus basin, we find emission intensity associated with fuel gas use in the Permian basin is 1.1341gCO_2/MJ.

Methane

The calculation equation of exhaust emission intensity in the Permian basin is similar to that in the Marcellus basin and is given by:

$$EI_{\text{tran-exhaust emission, } CH_4}$$

$$= \frac{\left(\sum\frac{(Number\ of\ compressor\ station)(Operating\ hour)(housepower)(EF\ of\ exhaust\ emission)}{Thermal\ efficiency}\right)}{(Natural\ gas\ throughput)}$$

$$= \frac{\left(\frac{8*10942hp*2890hr*3.7\frac{g\ CH_4}{hp\cdot hr}}{44\%}+\frac{3*18988\ hp*2587\ hr*0.031\frac{g\ CH_4}{hp\cdot hr}}{26\%}\right)\left(36\frac{g\ CO_2e}{g\ CH_4}\right)}{\left(1.24\times10^8\frac{Mcf}{facility\cdot year}\right)\left(1000\frac{scf}{Mcf}\right)\left(1036\frac{Btu}{scf}\right)\left(0.001055\frac{MJ}{Btu}\right)}$$

$$= 0.5698\ gCO_2e/MJ \quad \text{(S31)}$$

The procedure for calculating fugitive and venting emission intensities in the Permian basin is similar to that in the Marcellus basin. The parameters used for calculation and calculated fugitive and venting emission intensities for the Permian basin are shown in Table S12.

Table S12. Fugitive and venting emission intensities at the transmission stage for the Permian basin

Methane emission source	Parameters	Value	Data source	Emission intensity (gCO_2e/MJ)
Transmission station fugitives	Station fugitives (Mg CH_4/station)	64	Zimmerle et al. (2015)[23]	0.9508
	Reciprocating compressor fugitives (Mg CH_4/compressor)	64		
	Number of reciprocating compressors	8	Engineering based calculation	
	Centrifugal compressor fugitives (Mg CH_4/compressor)	54.5	Zimmerle et al. (2015)[23]	
	Number of centrifugal compressors	3	Engineering based calculation	
	Uncategorized fugitives (Mg CH_4/station)	200	Zimmerle et al. (2015)[23]	
Pipeline fugitives	Pipeline fugitives (kg CH_4/mile)	1120	GHGRP data[18,19,22]	0.0164
	Transmission distance (mile)	600		
Pneumatic devices venting	Pneumatic devices venting (Mg CH_4/device)	1	Zimmerle et al. (2015)[23]	0.0467
	Number of pneumatic devices	16	Assumption	
Transmission station venting	Station venting (Mg CH_4/station)	57	Zimmerle et al. (2015)[23]	0.1665
Pipeline venting	Pipeline venting (ton CH_4/year for 10,100 miles pipeline)	3810	GHGRP data[18,19,22]	0.0055
	Transmission distance (mile)	600		

S 5. Liquefaction stage emission inventory

The pipeline gas from both Marcellus and Permian basins is transported to the Sabine Pass Liquefaction facility to further remove impurities and be condensed to liquefied natural gas. In our study, we used the specific data from the Roman-White et al.[22], which is derived from the 2018 GHGRP subpart W and subpart C data for Chenier's Sabine pass liquefaction facility. Then, we adopted the average data of 10 liquefaction facilities from around the world in Nie et al.[27] to quantify the emission from power usage for ship at berth. As for the CO_2 venting from the acid gas removal unit, it is assumed that all emitted CO_2 is impurities removed from input pipeline quality gas.

S 5.1 Marcellus basin

The carbon dioxide and methane emission intensities at liquefaction stage for Marcellus basin are shown in Table S13 Table S14, respectively.

Carbon dioxide

Carbon dioxide emissions from fuel gas combustion and power use: The emission intensity of fuel gas combustion is calculated based on GHGRP Subpart C[18,19,22], which includes most emissions from the combustion of natural gas in a gas turbine and emissions from running thermal oxidizers. The emission intensity of fuel gas combustion in the Sabine Pass Liquefaction is shown:

$$\mathrm{EI}_{\text{lique-fuel use, } CO_2} = \frac{(Emission\ from\ NG\ combustion)}{(NG\ throughput)}$$

$$= \frac{(4.03 \times 10^6 \frac{ton\ CO_2}{year})(10^6 \frac{gCO_2}{ton})}{(1.02 \times 10^9 \frac{Mcf}{year})(1000 \frac{scf}{Mcf})(1036 \frac{Btu}{scf})(0.00105 \frac{MJ}{Btu})}$$

$$= 3.6147\ gCO_2/MJ \quad \text{(S32)}$$

The emission data for power use for ship at berth is obtained from Nie et al. work[27]. The carbon dioxide emission intensity for power use is 0.2370gCO_2/MJ.

Carbon dioxide emissions from acid gas removal: In the acid gas removal unit, the carbon dioxide extracted from the natural gas is assumed to be emitted into the atmosphere. And we assume that the adsorption efficiency is ideally 100%. All carbon dioxide is removed and the residual carbon dioxide concentration in the natural gas is to be zero. Since the CO_2 concentration in northeastern produced natural gas is zero[2], the carbon dioxide emission intensity from the acid gas removal unit is zero.

Carbon dioxide emissions from flaring: The flaring emission during the liquefaction facility is obtained directly from GHGRP Subpart W[18,19,22], which includes fugitives and flaring. The CO_2 emission intensity of flaring is shown:

$$\mathrm{EI}_{\text{lique-flaring, } CO_2} = \frac{(Emission\ from\ flaring)}{(NG\ throughput)}$$

$$= \frac{(1.44 \times 10^5 \frac{ton\ CO_2}{year})(10^6 \frac{gCO_2}{ton})}{(1.02 \times 10^9 \frac{Mcf}{year})(1000 \frac{scf}{Mcf})(1036 \frac{Btu}{scf})(0.00105 \frac{MJ}{Btu})}$$

$$= 0.1291\ gCO_2/MJ \quad \text{(S33)}$$

Table S13. Carbon dioxide emission intensities for the liquefaction stage in the Marcellus basin

Carbon dioxide emission category	Emission description	Emission intensity (gCO_2/MJ)
Energy use	Fuel gas combustion	3.6147
	Power use	0.2370
Acid gas removal	Acid gas removal	0
Flaring	Flare stacks	0.1291

Methane

The methane emission from the liquefaction facility mainly comes from exhaust methane emissions during fuel gas combustion, flaring, and fugitive emissions.

Methane emissions from exhaust: The exhaust emission intensity of fuel gas combustion is calculated based on GHGRP Subpart C data[18,19,22]. The exhaust emission intensity is shown:

$$EI_{\text{lique-exhaust emission, } CH_4} = \frac{(Exhaust\ emission\ from\ reciprocating\ compressors + Exhaust\ emission\ from\ gas\ turbines)}{(NG\ throughput)}$$

$$= \frac{((14 + 75.9) \frac{ton\ CH_4}{year})(10^6 \frac{gCH_4}{ton})(36 \frac{gCO_2e}{gCH_4})}{(1.02 \times 10^9 \frac{Mcf}{year})(1000 \frac{scf}{Mcf})(1036 \frac{Btu}{scf})(0.00105 \frac{MJ}{Btu})}$$

$$= 0.0029\ gCO_2e/MJ \quad \text{(S34)}$$

Methane emissions from leaks and flaring: The fugitives and flaring emission intensities are calculated based on GHGRP Subpart W[18,19,22].The flaring emission intensity is shown:

$$EI_{\text{lique-flaring, } CH_4} = \frac{(Emission\ from\ flaring)}{(NG\ throughput)}$$

$$= \frac{(4.92 \times 10^2 \frac{ton\ CH_4}{year})(10^6 \frac{gCH_4}{ton})(36 \frac{gCO_2e}{gCH_4})}{(1.02 \times 10^9 \frac{Mcf}{year})(1000 \frac{scf}{Mcf})(1036 \frac{Btu}{scf})(0.00105 \frac{MJ}{Btu})}$$

$$= 0.0159\ gCO_2e/MJ \quad \text{(S35)}$$

The fugitive emission intensity is shown:

$$\mathrm{EI}_{\text{lique-fugitives, } CH_4} = \frac{(Emission\ from\ fugitives)}{(NG\ throughput)}$$

$$= \frac{(3.99 \times 10^2 \frac{ton\ CH_4}{year})(10^6 \frac{g\ CH_4}{ton})(36 \frac{g\ CO_2e}{g\ CH_4})}{(1.02 \times 10^9 \frac{Mcf}{year})(1000 \frac{scf}{Mcf})(1036 \frac{Btu}{scf})(0.00105 \frac{MJ}{Btu})}$$

$$= 0.0129\ gCO_2e/MJ \quad \text{(S36)}$$

Table S14. Methane emission intensities for the liquefaction stage in the Marcellus basin

Methane emission category	**Emission description**	**Emission intensity (gCO_2e/MJ)**
Exhaust	Fuel gas combustion	0.0029
Leaks and flaring	Liquefaction leaks	0.0159
	Flare stacks	0.0129

S 5.2 Permian basin

The carbon dioxide and methane emission intensities at liquefaction stage for Permian basin are exactly same as that in Marcellus basin, shown in Table S15 Table S16, respectively.

Table S15. Carbon dioxide emission intensities for the liquefaction stage in the Permian basin

Carbon dioxide emission category	**Emission description**	**Emission intensity (gCO_2/MJ)**
Energy use	Fuel gas combustion	3.6147
	Power use	0.2370
Acid gas removal	Acid gas removal	1.1949
Flaring	Flare stacks	0.1291

Table S16. Methane emission intensities for the liquefaction stage in the Permian basin

Methane emission category	**Emission description**	**Emission intensity (gCO_2e/MJ)**
Exhaust	Fuel gas combustion	0.0029
Leaks and flaring	Liquefaction leaks	0.0159
	Flare stacks	0.0129

S 6. Shipping stage emission inventory

The shipping distance of each specific LNG supply chain is obtained from the shipping distance calculator website[28], as shown in Table S17. In order to analyze the effect of LNG tanker evolution, we included two types of LNG tanker. One is a traditional steam propulsion (steam) tanker (Abadi Brunei Gas Carriers

Mitsubishi) with a capacity of 137,000 m^3. Another is a dual-fuel low pressure propulsion (X-DF) tanker (Celsius Canberra Celsius Shipping Samsung) with a capacity of 180,000m^3. The result in the main text is based on steam LNG tanker. The calculation of shipping emission intensities is based on Rosselot et al. model,[29] where both the boil-off gas (BOG) generation rate and the ratio of methane slip to BOG are obtained from the first measurement campaign on an LNG carrier.[30] If it is not specified, all following parameters and calculations are for Marcellus-UK and Permian-UK supply chains.

Table S17. The shipping distance of each supply chain

LNG supply chain	**Distance (nm)**
Marcellus-UK	4,520
Marcellus-China	9,966
Permian-UK	4,520
Permian-China	9,966

S 6.1 Steam powered

All the carbon dioxide emission during the shipping stage comes from combustion of BOG. BOG has three primary fates: combustion in generators not associated with propulsion; combustion in propulsion systems; combustion in gas combustion units (GCU). The details of assigning the BOG to its combustion destination refere to Rosselot et al. work.[31] The estimated BOG generation rate for each modeled category of journey (underway, maneuvering, and docked) is multiplied by adjustment factors to arrive at an estimate of BOG generation for a specific carrier other than the measured one. The BOG generation rate and the ratio of methane slip to BOG at each modeled category of journey are shown in Table S18 and Table S19. Other parameters regarding the characteristic of LNG tanker and LNG are shown in Table S20.

Table S18. BOG generation rate at each modeled category of journey[29]

	Underway (t CO_2/ km)	**Maneuvering (t CO_2/day)**	**Docked (t CO_2/day)**
Generators	1.9636E-2	1.6488E+01	1.9659E+01
Propulsion	6.0674E-02	0.0000E+00	0.0000E+00
GCU	0.0000E+00	2.6194E+01	5.3061E+00
Overall	8.0310E-02	4.2682E+01	2.4965E+01

Table S19. The ratio of methane slip to BOG at each modeled category of journey[29] for steam tanker

	Underway (t CH_4/ km)	**Maneuvering (t CH_4/day)**	**Docked (t CH_4/day)**
Generators	8.3405E-02	8.2058E-02	8.7863E-02
Propulsion	5.0000E-05	0.0000E+00	0.0000E+00
GCU	0.0000E+00	0.0000E+00	0.0000E+00

Table S20. Other parameters regarding the characteristic of steam powered LNG tanker and LNG

Shipping distance (km)	16742

Number of days spent maneuvering	1.7
Number of days docked (for loading, unloading, refueling)	3.3
Containment technology adjustment factor for Abadi Brunei Gas carriers Mitsubishi	1.88
Surface area adjustment factor for Abadi Brunei Gas carriers Mitsubishi	0.85267
Tanker cargo capacity (m^3)	137000
Ballast remaining in containment after unloading at destination (% of carrier capacity)	2.5%
Heating value of LNG in gas phase (Btu/scf)	1036
Density of LNG in gas phase (kg/m^3)	0.68
Density of LNG at Sabine Pass Liquefaction (kg/m^3)	431
Mass fraction of methane in LNG	0.916
Moles C per mole LNG	1.049
MW of pipeline gas	16.729
MW of carbon dioxide	44.010

The amount of generated BOG is calculated by multiplying the generation rate and corresponding shipping distance or operating days, as shown in Table S21. In this study, the emissions are estimated based on a round trip. The methane emissions is calculated by multiplying the ratio of methane slip to BOG and amount of generated BOG, as shown in Table S22.

Table S21. BOG generation at each modeled category of journey in steam powered LNG tanker

	Underway ($t CO_2$)	**Maneuvering ($t CO_2$)**	**Docked ($t CO_2$)**
Generators	526.99	44.93	103.99
Propulsion	1628.36	0.00	0.00
GCU	0.00	71.38	28.07

Table S22. Methane generation at each modeled category of journey in steam powered LNG tanker

	Underway ($t CH_4$)	**Maneuvering ($t CH_4$)**	**Docked ($t CH_4$)**
Generators	43.95	3.69	9.14
Propulsion	0.08	0.00	0.00
GCU	0.00	0.00	0.00

Carbon dioxide emissions: The emission intensity of is given by:

$$EI_{\text{ship-BOG combustion, } CO_2} = \frac{(BOG\ generated - CH_4\ slip)(Mole\ C\ per\ LNG)(\frac{MW\ of\ CO_2}{MW\ of\ pipelien\ gas})}{(LNG\ capacity)(1 - Ballast\ remaining)(Heating\ value\ of\ NG)}$$

$$= \frac{(2403.73\ ton\ NG - \frac{56.86\ ton\ CH4}{0.916})(1.049\frac{Mole\ C}{Mole\ NLG})(\frac{44.010}{16.729})(1000000\frac{g}{ton})}{(137000\ m^3\ LNG)(1-2.5\%)(\frac{431\ \frac{kg\ LNG}{m^3}}{0.68\ \frac{kg\ LNG}{m^3}})(35.3\frac{scf}{m^3})(1036\frac{Btu}{scf})(0.001055\frac{MJ}{Btu})}$$

$$= 1.9780\ gCO_2/MJ \quad \text{(S37)}$$

The above calculation is repeated by employing different shipping distances. Finally, we obtained the carbon dioxide emission intensities for each LNG supply chain, as shown in Table S23.

Table S23. CO_2 emission intensities for steam powered LNG tanker along each LNG supply chain

LNG supply chain	**CO_2 emission intensity (gCO_2/MJ)**
Marcellus-UK	1.9780
Marcellus-China	4.1228
Permian-UK	1.9780
Permian-China	4.1228

Methane emissions: The emission intensity of is given by:

$$\text{EI}_{\text{ship-methane slip, } CH_4} = \frac{(Total\ methane\ slip)(GWP\ of\ CH4)}{(LNG\ capacity)(1-Ballast\ remaining)(Heating\ value\ of\ NG)}$$

$$= \frac{(56.86\ ton\ CH_4)(1000000\frac{g}{ton})(36\frac{g\ CO_2e}{g\ CH_4})}{(137000\ m^3\ LNG)(1-2.5\%)(\frac{431\ \frac{kg\ LNG}{m^3}}{0.68\ \frac{kg\ LNG}{m^3}})(35.3\frac{scf}{m^3})(1036\frac{Btu}{scf})(0.001055\frac{MJ}{Btu})}$$

$$= 0.6266\ gCO_2e/MJ \quad \text{(S38)}$$

We use different shipping distances and repeated the above calculation process. Finally, we obtained the methane emission intensities for each LNG supply chain, as shown in Table S24.

Table S24. Methane emission intensities for steam powered LNG tanker along each LNG supply chain

LNG supply chain	**Methane emission intensity (gCO_2e/MJ)**
Marcellus-UK	0.6266
Marcellus-China	1.2113
Permian-UK	0.6266
Permian-China	1.2113

S 6.2 X-DF powered

Carbon dioxide

All the carbon dioxide emission during the shipping stage comes from combustion of BOG. Same as that in steam powered LNG tanker, BOG also has three primary fates: combustion in generators not associated with propulsion; combustion in propulsion systems; combustion in gas combustion units (GCU). The estimated BOG generation rate for each modeled category of journey (underway, maneuvering, and docked) is multiplied by adjustment factors to arrive at an estimate of BOG generation for a specific carrier other than the measured one. The BOG generation rate for X-DF powered LNG tanker is same as that for steam powered LNG tanker, as shown in Table S18. The ratio of methane slip to BOG for X-DF powered LNG tanker is shown in Table S25. Other parameters regarding the characteristic of X-DF powered LNG tanker and LNG are shown in Table S26.

Table S25. The ratio of methane slip to BOG at each modeled category of journey[29] for X-DF tanker

	Underway (t CH_4/ km)	**Maneuvering (t CH_4/day)**	**Docked (t CH_4/day)**
Generators	8.3405E-02	8.2058E-02	8.7863E-02
Propulsion	2.1858E-02	0.0000E+00	0.0000E+00
GCU	0.0000E+00	0.0000E+00	0.0000E+00

Table S26. Other parameters regarding the characteristic of X-DF powered LNG tanker and LNG

Shipping distance (km)	16742
Number of days spent maneuvering	1.7
Number of days docked (for loading, unloading, refueling)	3.3
Containment technology adjustment factor for Abadi Brunei Gas carriers Mitsubishi	1.0
Surface area adjustment factor for Abadi Brunei Gas carriers Mitsubishi	1.0229
Tanker cargo capacity (m^3)	180000
Ballast remaining in containment after unloading at destination (% of carrier capacity)	2.5%
Heating value of LNG in gas phase (Btu/scf)	1036
Density of LNG in gas phase (kg/m^3)	0.68
Density of LNG at Sabine Pass Liquefaction (kg/m^3)	431
Mass fraction of methane in LNG	0.916
Moles C per mole LNG	1.049
MW of pipeline gas	16.729
MW of carbon dioxide	44.010

The amount of generated BOG is calculated by multiplying the generation rate and corresponding shipping distance or operating days, as shown in Table S27. In this study, the emissions are estimated based on a round trip. The methane emissions are calculated by multiplying the ratio of methane slip to BOG and amount of generated BOG, as shown in Table S28.

Table S27. BOG generation at each modeled category of journey in X-DF powered LNG tanker

	Underway ($t CO_2$)	Maneuvering ($t CO_2$)	Docked ($t CO_2$)
Generators	336.26	28.67	66.36
Propulsion	1039.03	0.00	0.00
GCU	0.00	45.55	17.91

Table S28. Methane generation at each modeled category of journey in X-DF powered LNG tanker

	Underway ($t CH_4$)	Maneuvering ($t CH_4$)	Docked ($t CH_4$)
Generators	28.05	2.35	5.83
Propulsion	22.71	0.00	0.00
GCU	0.00	0.00	0.00

Carbon dioxide emissions: The emission intensity of is given by:

$$\mathrm{EI}_{\text{ship-BOG combustion, } CO_2} = \frac{(BOG\ generated - CH_4\ slip)(Mole\ C\ per\ LNG)(\frac{MW\ of\ CO_2}{MW\ of\ pipelien\ gas})}{(LNG\ capacity)(1 - Ballast\ remaining)(Heating\ value\ of\ NG)}$$

$$= \frac{(1553.78\ ton\ NG - \frac{58.94\ ton\ CH4}{0.916})(1.049\frac{Mole\ C}{Mole\ NLG})(\frac{44.010}{16.729})(1000000\frac{g}{ton})}{(180000\ m^3\ LNG)(1 - 2.5\%)(\frac{431\ \frac{kg\ LNG}{m^3}}{0.68\ \frac{kg\ LNG}{m^3}})(35.3\frac{scf}{m^3})(1036\frac{Btu}{scf})(0.001055\frac{MJ}{Btu})}$$

$$= 0.9643\ gCO_2/MJ \quad \text{(S39)}$$

The above calculation is repeated by employing different shipping distances. Finally, we obtained the carbon dioxide emission intensities for each LNG supply chain, as shown in Table S29.

Table S29. CO_2 emission intensities for steam powered LNG tanker along each LNG supply chain

LNG supply chain	CO_2 emission intensity (gCO_2/MJ)
Marcellus-UK	0.9447
Marcellus-China	1.9671
Permian-UK	0.9447
Permian-China	1.9671

Methane emissions: The emission intensity of is given by:

$$\mathrm{EI}_{\text{ship-methane slip, } CH_4} = \frac{(Total\ methane\ slip)(GWP\ of\ CH4)}{(LNG\ capacity)(1 - Ballast\ remaining)(Heating\ value\ of\ NG)}$$

$$= \frac{(58.94\ ton\ CH_4)(1000000\frac{g}{ton})(36\frac{g\ CO_2e}{g\ CH_4})}{(180000\ m^3\ LNG)(1-2.5\%)(\frac{431\ \frac{kg\ LNG}{m^3}}{0.68\ \frac{kg\ LNG}{m^3}})(35.3\frac{scf}{m^3})(1036\frac{Btu}{scf})(0.001055\frac{MJ}{Btu})}$$

$$= 0.4944\ gCO_2e/MJ \quad \text{(S40)}$$

We use different shipping distances and repeat the above calculation process. Finally, we obtained the methane emission intensities for each LNG supply chain, as shown in Table S30.

Table S30. Methane emission intensities for steam powered LNG tanker along each LNG supply chain

LNG supply chain	**Methane emission intensity (gCO_2e/MJ)**
Marcellus-UK	0.4944
Marcellus-China	1.0073
Permian-UK	0.4944
Permian-China	1.0073

S 7. Energy flow from upstream through shipping stage

Figure S3 shows the energy flow along Marcellus-CN and Permian-CN LNG supply chains. The energy entering each stage of the gas is calculated from backward to forward according to the energy conservation law. The function unit assumed in our paper is 1M J (equal to 1000 kJ) of natural gas delivered to the destination country. Based on the known emission data and fuel gas combustion data for each process, we can calculate the energy loss in each stage due to emission and fuel gas combustion. The energy output of a stage plus the energy loss from fuel gas combustion and methane leakage equals the input to this stage. Co-products such as upstream hydrocarbon liquids (including crude oil and lease condensate) and processing hydrocarbon liquids (including processing plant condensate and NGLs) are removed from the supply chain at the upstream and processing stages. The energy content of these co-products removed from the supply chain is quantified based on the fractions of processing hydrocarbon liquids in produced gas and upstream hydrocarbon liquids in produced hydrocarbon. The details about emission allocation are shown in S8.

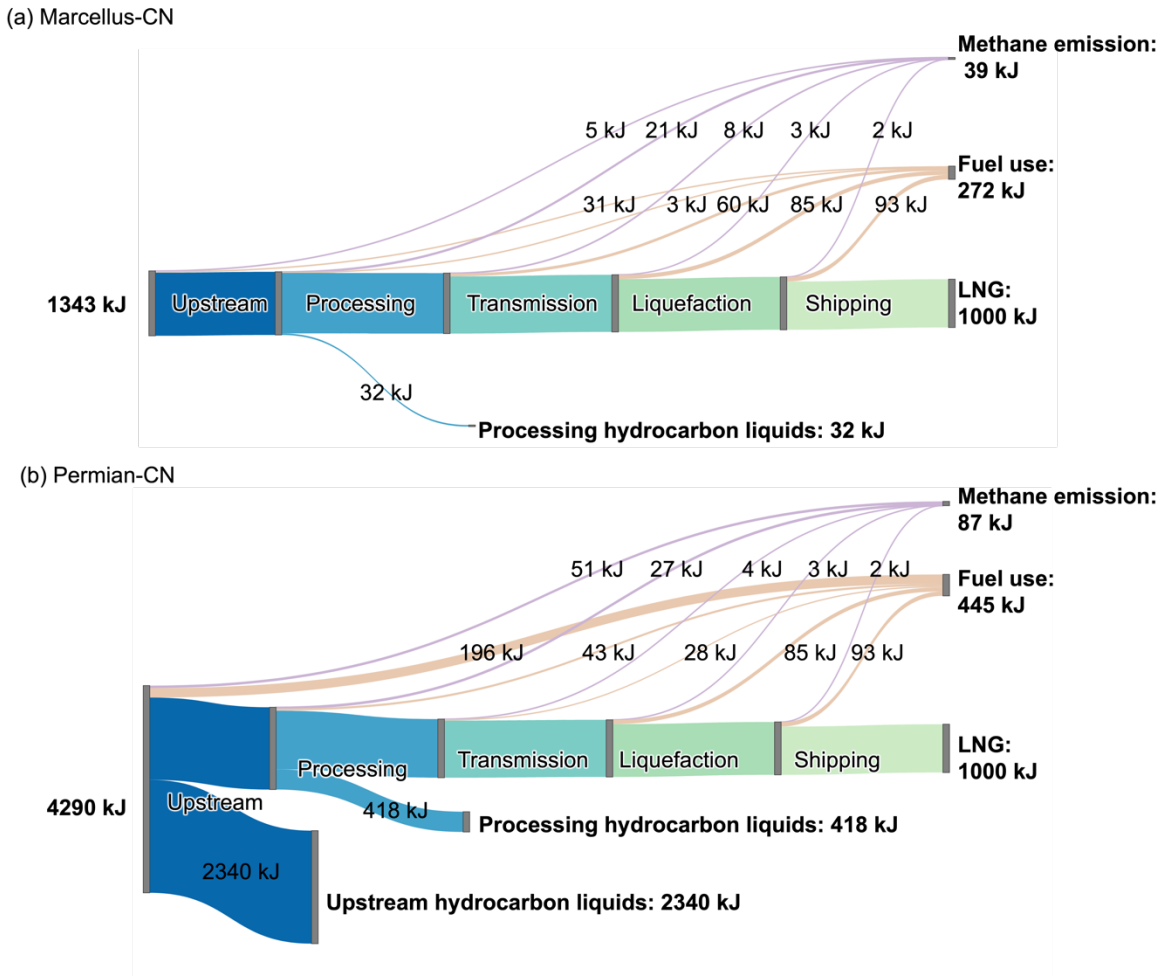

Figure S3. Energy flow along (a) Marcellus-China LNG supply chain, and (b)Permian-China LNG supply chain.

The Marcellus-China LNG supply chain is used as an example to illustrate the above calculation procedure. As shown in following equation, the energy loss caused by fuel gas combustion during the shipping process is 0.0848 MJ/(MJ NG in shipping), and the energy loss due to methane slip during natural gas combustion is 0.0021 MJ/(MJ NG in shipping input). Given 1 MJ of LNG delivered, the energy needed to enter the shipping stage is 1.0951 MJ. The similar calculation is repeated for all stages to obtain the energy loss intensity and energy entering each stage. The energy loss caused by fuel gas combustion and methane emissions during the liquefaction are 0.0721 and 0.0026 MJ/(MJ NG in liquefaction input), and the calculated energy entering into liquefaction stage is 1.1835 MJ. The energy loss caused by fuel gas combustion and methane emissions during the transmission are 0.0481 and 0.0064 MJ/(MJ NG in transmission input), and 1.2516 MJ of pipeline dry gas is outputted from processing stage, entering into transmission stage. Since the energy-based fraction of NGLs in produced gas is 2.5%, the energy of the processing hydrocarbon liquids removed from the processing plant is 0.0321 MJ. The energy loss due to

fuel consumption and methane emissions during the processing stage is 0.0178 MJ/(MJ NG in processing input), and the energy entering into the processing stage is 1.3070 MJ. The energy loss due to fuel consumption and methane emissions during the upstream stage is 0.0272 MJ/(MJ NG in upstream input), and the energy entering into the upstream stage is 1.3436 MJ.

According to Figure S3, for 1 MJ of LNG delivered at the destination port, the Marcellus basin only needs to produce 1.343 MJ of hydrocarbon at the upstream stage, while the Permian basin needs to produce 4.290 MJ of hydrocarbons.

The energy loss caused by fuel gas combustion from steam tanker during shipping along Marcellus-China supply chain is given by:

$$\mathrm{EL}_{\text{ship-BOG combustion, } CO_2} = \frac{(BOG\ generated - CH_4\ slip)(Heating\ value\ of\ NG)}{(LNG\ capacity)(1 - Ballast\ remaining)(Heating\ value\ of\ NG)}$$

$$= \frac{(5000.65\ ton\ NG - \frac{109.92\ ton\ CH4}{0.916})(1000\frac{kg}{ton})(\frac{1}{0.68}\frac{m^3}{kg})(35.3\frac{scf}{m^3})(1036\frac{Btu}{scf})(0.001055\frac{MJ}{Btu})}{(137000\ m^3\ LNG)(1 - 2.5\%)(\frac{431\ \frac{kg\ LNG}{m^3}}{0.68\ \frac{kg\ LNG}{m^3}})(35.3\frac{scf}{m^3})(1036\frac{Btu}{scf})(0.001055\frac{MJ}{Btu})}$$

$$= 0.0848\frac{MJ\ energy\ loss}{MJ\ gas\ into\ shipping} \quad \text{(S41)}$$

The energy loss caused by the methane leakage from steam tanker during the shipping stage along Marcellus-China supply chain is given by:

$$\mathrm{EL}_{\text{ship-methane slip, } CH_4} = \frac{(Total\ methane\ slip)(Heating\ value\ of\ NG)}{(LNG\ capacity)(1 - Ballast\ remaining)(Heating\ value\ of\ NG)}$$

$$= \frac{(\frac{109.92\ ton\ CH_4}{0.916})(1000\frac{kg}{ton})(\frac{1}{0.68}\frac{m^3}{kg})(35.3\frac{scf}{m^3})(1036\frac{Btu}{scf})(0.001055\frac{MJ}{Btu})}{(137000\ m^3\ LNG)(1 - 2.5\%)(\frac{431\ \frac{kg\ LNG}{m^3}}{0.68\ \frac{kg\ LNG}{m^3}})(35.3\frac{scf}{m^3})(1036\frac{Btu}{scf})(0.001055\frac{MJ}{Btu})}$$

$$= 0.0021\frac{MJ\ energy\ loss}{MJ\ gas\ into\ shipping} \quad \text{(S42)}$$

S 8. Emission allocation

In this study, we employ an energy-based and product-assigned allocation method to handle the co-production of crude oil, lease condensate, processing plant condensate, NGLs, and dry gas in the upstream and processing stages. First, all co-products related to a specific process are identified, and then the emissions associated with this process are assigned between co-products based on energy content. If the

emission from a process is only related to dry gas, then we would assign emissions wholly to it. As shown in Figure S4, there is a two-step emission allocation in this study. The first step occurs at the upstream stage, where emissions are allocated between crude oil, lease condensate, and produced gas. It should be noted that the emissions allocated to produced gas should be further allocated between processing plant condensate, NGLs and dry gas because we only consider the emissions associated with LNG, the final form of dry gas. Then in the second step, the emissions are allocated between processing plant condensate, NGLs, and dry gas. Therefore, the key to allocation is to calculate energy-based fractions of each products by employing appropriate production data over the study region.

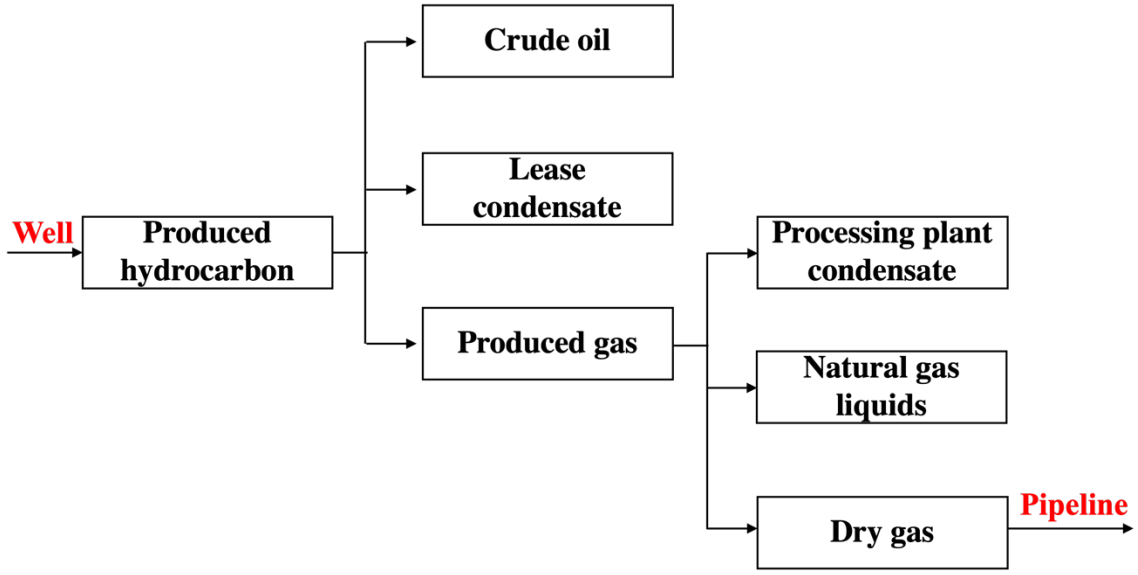

Figure S4. Two-step emission allocation process

Based on the available production and heating value data for all products in Permian basin (Table S31), the energy fraction for each product is calculated, as shown in Table S33. For the Marcellus basin, the crude oil, lease condensate and produced gas production is obtained from Department of Environmental Protection (DEP) in Pennsylvania. The production data is provided by county. Table S32 shows the aggregated production data across all dry gas production counties in the northeaster Marcellus, including Westmoreland, Centre, Fayette, Lycoming, Clearfield, Wyoming, Susquehanna, Huntingdon, Bradford, Indiana, Armstrong, McKean, Sullivan, Tioga, Jefferson, Somerset, Elk, Cameron, Cambria, Clinton, Potter, Blair, Bedford. Since there is no specific NGLs, processing plant condensate and dry gas production data for northeastern Marcellus, we use the energy fraction of methane in produced gas to approximate the energy fraction of dry gas in produced gas, which is shown in Table S33.

Table S31. Production rates and heating values for all products in the Marcellus basin.

Category	Item	Production [a]	Heating value [b]
Crude oil	Crude oil	0	5.8
Lease condensate	Lease condensate	1	4.88
Produced gas	Produced gas	12745	1023.1

a. The production unit for all products are bbl/day, except for produced gas, which is in MMcf/day.

b. The heating value unit for all products are MMBtu/bbl, except for produced gas, which is in Btu/scf.

Table S32. Production rates and heating values for all products in the Permian basin. The production data are obtained from Rosselot et al. study,[12] which is originally from Texas Railroad commission (TRCC) and New Mexico Oil Conservation Division (NMOCD).[7,9,10] The heating values for all products are also obtained from Rosselot et al. study,[12] except for produced gas, which is calculated based on the produced gas composition data in that region. [17]

Category	Item	Production [a]	Heating value [b]
Crude oil	Crude oil	3157452	5.8
Lease condensate	Lease condensate	369266	4.88
Produced gas	Produced gas	11579	1224.5
Processing plant condensate	Condensate from processing plant	42026	4.88
	Other hydrocarbon liquids produced from produced gas	263892	4.9
NGLs	Natural gasoline	80752	4.62
	Butane and propane	286873	3.99
	Ethane	232612	2.64

a. The production unit for all products are bbl/day, except for produced gas, which is in MMcf/day.

b. The heating value unit for all products are MMBtu/bbl, except for produced gas, which is in Btu/scf.

Table S33. Energy fraction of each product in both Marcellus and Permian basins.

Basin	Crude oil	Lease condensate	Produced gas					
			Processing plant condensate		NGLs			Dry gas
			Condensate from processing	Other hydrocarbon liquids	Natural gasoline	Butane and propane	Ethane	Dry gas
Marcellus	0.0%	0.0%	2.5%					97.5%
Permian	52.5%	5.4%	0.6%	3.8%	1.1%	3.4%	1.8%	31.3%

S 9. Summary of measured methane leakage rate

Table S34 is a summary of measurements campaigns over Marcellus and Permian basin. In general, the Marcellus basin has lower emission rates than that in Permian basin.

In Caulton et al., an aerial measurement was conducted in June, 2012 over southwestern PA using Purdue's Airborne laboratory for Atmospheric Research, a modified Beechcraft Duchess aircraft equipped with a 0.5-Hz high precision Picarro $CO_2/CH_4/H_2O$ cavity ring down spectrometer. In their study, an original sampling area (OSA) used for aircraft flux calculation and a bottom-up inventory is defined by the bounding longitude coordinates −80.6405 to −79.9315 and the bounding latitude coordinates 40.1475 to 39.7217, with a total area of 2844 km^2. In order to investigate the influence of advective transport from the upwind area, an upwind accumulation area (UAA) is calculated by NOAA Hybrid Single Particle Lagrangian Integrated Trajectory Model (HYSPLIT), covering 14597 km^2. The average emissions over the entire 18-hr back trajectory region (UAA) corresponds to a lower limit for the bottom-up flux, while the 5 to 6-hr estimates in OSA represents an upper limit for comparison with the bottom-up flux. In the OSA region, the top-down measured flux is 2-4.2 g $CH_4/s/km^2$. The natural gas production rate in that region is 15.9 $gCH_4/s/km^2$. The fraction of production (including flowback) is calculated based on inventory estimates assuming Howarth et al., ranging from 5.2-19.8%. Therefore, the measured CH_4 emission rate is 0.65-5.22 %. Similarly, in the UAA region, the top-down measured flux is 6.6-14 g $CH_4/s/km^2$. The natural gas production rate in that region is 50.1 $gCH_4/s/km^2$. Based on the calculated fraction of production 5.2-19.8%, the measured CH_4 emission rate is 0.68-5.53 %. In summary, the measured CH_4 emission rate for production stage is 0.65-5.53%. The CH_4 production rate in the UAA region is 2.63 Gg/hr.

In Peischl et al., they estimated the total CH_4 emission to the atmosphere from Northeastern Pennsylvania using measurements taken aboard the chemically instrumented National Oceanic and Atmospheric Administration (NOAA) WP-3D aircraft in the summer of 2013 during the Southeast Nexus (SENEX) field campaign. The quantification of CH4 emissions is based on mass balance approach. The reported CH_4 flux associated with natural gas production in the measured region in Marcellus is $(1.56\pm0.6)\times10^7$ g/h. The reported natural gas production is calculated to be $(18 \pm 1) \times 10^7$ m^3 of natural gas per day based on the production data from EIA and Pennsylvania Department of Environmental protection Web site. Based on the methane content in natural gas (96±3)%, the natural gas loss rate is 0.18-0.41%. However, this natural gas loss rate sources from serval processes, including upstream natural gas extraction, processing, and compression operations. There is no clear emission allocation among these processes. Therefore, the calculated total natural gas loss rate is not applicable in our study.

In Omara et al., the downwind tracer flux measurements approach is employed to measure facility-level CH_4 emissions from conventional and unconventional sites across the Marcellus basin. The results show that absolute facility-level CH_4 emission rates were highest among the flowback and unconventional natural gas sites and lowest among the conventional natural gas sites. However, on a production-normalized basis (CH_4 emitted as a fraction of total CH_4 produced), conventional sites generally had higher production-normalized CH_4 emission rates (median: 10.5%; range: 0.35-91%) compared to unconventional sites (median: 0.13%, range: 0.01-1.2%). In the measured region, the unconventional natural gas production is 4.8 billion Mcf, while the conventional natural gas production is only 0.272 billion Mcf, accounting for 5.4% of total natural gas production.

In Barkley et al., two different top-down methodologies are employed to quantify CH_4 emissions coming from upstream stage (unconventional wells and compressor stations) within 41.1-42.2 ◦ N 75.2-77.6◦ W. In this region, despite the large number of wells, the average conventional well in PA produces 1% of the natural gas of its unconventional counterpart. One of the methods is collecting 10 individual flights over a 3-week period in May 2015 based on mass balance approach. The other is simulating the CH_4 emission enhancements by inputting compiled inventory for the region into atmospheric transport model. The aerial measured average CH_4 emission across all flights are 0.40% for mean, with a 2σ confidence interval between 0.08 and 0.72 % of production. The average CH_4 production in the measurement box is 4.6 Gg/hr.

In Robertson et al., methane emission fluxes were estimated for 71 oil and gas well pads in Delaware basin by using a mobile laboratory and inverse Gaussian dispersion method. Measurements were performed using the University of Wyoming Atmospheric Science Mobil Research Laboratory. In the measurements, a Picarro Cavity Ringdown Spectrometer was used to measure methane and water vapor mixing ratios and the wind sensor, sonic anemometer and weather station were installed on the mast of the Mobil Lab to obtain meteorological data. In this study, sites with emissions that were below detection limit were recorded and included in the sample. Average emission rate per site was estimated by bootstrapping and by maximum likelihood best log-normal fit. Finally, the estimated methane emission rate over Delaware basin is 3.76 kg/hr (range: 2.24-5.71 kg/hr). Normalized to gross gas production 762 Mcf (range: 435-1210 Mcf) in that region, the methane emission rate is 0.89% (range: 0.42-1.83%).

In Zhang et al., based on TROPOMI satellite observations and atmospheric inverse modeling, the methane emissions from the Permian basin (29°-34° N, 100°-106° W) are reported. Based on satellite measurements from May 2018 to March 2019, Permian methane emission from oil and natural gas production are estimated to be 2.7 ± 0.5 Tg/year, which is approximately one quarter of total emissions

from all U.S. oil and gas production areas in 2015 (10.9 Tg/year, including emission from production, gathering, and processing, which largely occur in the production areas). Given the methane production rate 73 Tg CH_4/year(derived from 127 billion m^3/year natural gas production during the study period using 80% methane content by volume), the production-normalized methane emission rate is calculated to be 3.7 ± 0.7%.

In Irakulis-Loitxate et al., a satellite-based large-scale and high-resolution survey of methane point emitters in the Permian basin is conducted. The dataset was acquired by three satellite missions launched between 2018 and 2019: two versions of Advanced Hyperspectral Imager (AHSI) onboard China's Gaofen-5 (GF5) and ZYI satellites and the imaging spectrometer onboard Italy's PRISMA mission. The methane emission data is obtained for a ~150km-by-200km area in the Delaware basin during four different dates: 15 May 2019, 1 November 2019, 29 December 2019, and 8 February 2020. In this study, 19 plumes detected from one single overpass of the GF5-AHSI system on 8 February 2020. The resulting integrated flux from the Permian plumes is 0.28 Tg/year (0.2-0.35Tg/year). Since the minimum detection threshold of this satellite imaging spectroscopy is 500 kg/hr, the estimated methane emissions is very likely to underestimate the actual emissions.

In Cusworth et al., they conducted an extensive airborne campaign across the majority of the Permian basin in September-November 2019 with imaging spectrometers to quantify methane point source emissions at facility-scales. Two remote sensing airborne platforms is employed in this study, including the Next-Generation Airborne Visible/Infrared Imaging Spectrometer (AVIRIS-NG) and the Global Airborne Observatory (GAO). The GAO imaging spectrometer is identical to the AVIRIS-NG instrument and has the same performance. The measurement technologies are able to identify strong methane emission sources and attribute then to different emission sector (production, gathering and boosting, processing). The study region includes a 39000 km^2 area in Delaware basin and 16000 km^2 area in the Midland basin. The estimated methane emissions are 0.74 ± 0.24 Tg/year from production, 0.55 ± 0.19 from gathering and boosting, and 0.18 ± 0.05 from processing. One problem with this study is that the measurement technology has high minimum detection threshold, which may severely underestimate the actual emissions, especially at production sites.

In Chen et al., a basin-wide airborne survey across oil and gas extraction and transportation activities is conducted in the New Mexico Permian basin, spanning 35923 km_2. The aerial survey is performed by Kairos Aerospace to evaluate medium-to-large point-source emissions. The airborne survey repeatedly visited over 90% of the active wells in the survey region throughout October 2018 to January 2020. The detected CH_4 emission rate from the New Mexico Permian is 153 (+71/-70 95% CI) metric tones per hour

(t/hr). This corresponds to 7.4% ± 3.4% of gross gas production in the full survey area. Accounting for partial detection, emissions below minimum detection limit, and scaling up to assets not covered in this aerial campaign, the total survey area emission estimate is 194 (72/-68) t/hr, equivalent to 9.4% (+3.5%/-3.3%) of gross gas production. A breakdown of measured emission rate by emission source asset type indicates 51% of emissions from upstream, 36% from transmission, 6% storage, 3% processing plant, and 5% from ambiguous sources.

Table S34. Literature summary of methane emission measurements in Marcellus and Permian basin

Basin	**Author and published year**	**CH_4 leakage rate (% of total NG production if it is not specified)**	**Method**	**Site location**	**Facility coverage**
Marcellus	Caulton et al. (2014)[24]	Lower: 2.8% Upper: 16.4% (OSA)	Aerial spectrometer	Southwestern Marcellus	Production, processing, and transmission
		Lower: 2.9% Upper: 17.3% (UAA)			
	Peischl et al. (2015)[32]	Lower: 0.18% Upper: 0.41%	Aerial mass balance	Northeastern Marcellus	NG extraction, processing, and compressor operations
	Omara et al. (2016)[33]	Lower:0.35% Upper: 91%, median: 11% (Conventional)	Downwind tracer flux measurements	Southwestern Marcellus	Production (emissions from oil wells and NG wells in the drilling stage are not included)
		Lower: 0.01% Upper: 1.2% median:0.13% (Unconventional)			
	Barkley et al. (2017)[6]	Lower: 0.08% Upper: 0.72% Median: 0.4%	Aerial mass balance	Northeastern Marcellus	Production, gathering and boosting
Permian	Robertson et al. (2020)[34]	Lower: 0.42% Upper: 1.83% Median: 0.89%	Mobile laboratory and Gaussian dispersion method	Delaware basin	Production
	Zhang et al. (2020)[8]	Lower: 3.0% Upper: 4.4% Median: 3.7%	Satellite data	Whole Permian basin	Production, G&B, and processing
	Irakulis-Loitxate et al. (2021)[35]	0.28 Tg/year	Satellite data	Delaware basin	Production, G&B, and processing

	Cusworth et al. (2021)[36]	Production: 0.74±0.24 G&B: 0.55±0.19 Processing:0.18±0.05 (Unit: Tg/year)	Airborne imaging spectrometer	Delaware basin and Midland basin	Production, G&B, and processing
	Chen et al. (2022)[37]	Lower: 6.1% Upper: 12.9% Median: 9.4%	Aerial imaging spectrometer	Delaware basin	Production, G&B, and processing

Not all measurement studies can be incorporated into our LCA model. First, the selected studies should report measured methane emission rate specific to study region. Since our study region is northeastern Marcellus basin and whole Permian basin, we only consider Peischl et al. and Barkley et al. studies for northeastern Marcellus, Zhang et al. and Cusworth et al. studies for Permian basin. In addition, the selected studies should have clear emission allocation among included stages. Since the Peischl et al study doesn't have any emission allocation among the included stages (NG extraction, processing, and compressor operations), it cannot be directly used in our model. Finally, the selected studies should not exclude emissions from major process stages. In Cusworth et al. study, the high minimum detection threshold of their aerial measurements results in underestimation of emissions at production sites. Therefore, this study is not used in our LCA model. To sum up, the measurement from Barkley et al. is employed for northeastern Marcellus basin, and measurement from Zhang et al. is used for Permian basin.

Table S35. Measured methane emission distribution across different stages in Caulton et al.[24]

Source	Original Study Area		Upwind Accumulation Area	
	Expected emissions, $gCH_4/s/km^2$_low	Expected emissions, $gCH_4/s/km^2$_high	Expected emissions, $gCH_4/s/km^2$_low	Expected emissions, $gCH_4/s/km^2$_high
Natural gas	0.85	2.23	0.76	1.7
Production	0.15	0.95	0.05	0.3
Processing	0.11	0.11	0.03	0.03
Local trans/distr	0.28	0.55	0.28	0.58
Interstate trans/distr	0.31	0.62	0.4	0.81
Oil	0		0	
Coal	2.96		1.01	
Flowback	0.05	0.1	0.01	0.02
AFO	0.015		0.015	
Other	0		0.019	
Total	3.88	5.31	1.81	2.76
Contribution of processing	1.1%-2.8%			
Top down flux ($gCH_4/s/km^2$)	6.6	14	2	4.2

Natural gas production rate ($gCH_4/s/km^2$)	50.1	15.9
Production-normalized CH_4 emission rate (%)	0.14%-0.79%	

Table S36. Measured methane emission distribution among different stages in Zhang et al.[8]

	Production	Gathering and boosting	Processing
2018 GHGRP methane emissions, adjusted for produced gas throughput[12] (kg methane/year)	279383549	165834880	23166320
Contribution of each stage	60%	35%	5%
Total	Median: 3.7% (3.0%-4.4%)		
Production-normalized CH_4 emission rate (%)_median	2.22%	1.30%	0.19%
Production-normalized CH_4 emission rate (%)_lower	1.80%	1.05%	0.15%
Production-normalized CH_4 emission rate (%)_upper	2.64%	1.54%	0.22%

Table S37. Measured methane emission distribution among different stages in Chen et al.[37]

	Measured emission rate_median (t/hr)	Contribution of each process	Production-normalized CH_4 emission rate_median (%)	Production-normalized CH_4 emission rate_lower (%)	Production-normalized CH_4 emission rate_upper (%)
Well sites	79	51.3%	4.82%	3.13%	6.62%
Pipelines	29	18.8%	1.77%	1.15%	2.43%
Compressor stations without a well on site	26	16.9%	1.59%	1.03%	2.18%
Stand-alone storage tank sites	9	5.8%	0.55%	0.36%	0.75%
Gas processing plants	4	2.6%	0.24%	0.16%	0.34%
Ambiguous sources	7	4.5%	0.43%	0.28%	0.59%

Total measured emission rate	153	100.0%	9.40%	6.10%	12.90%

In the northeastern Marcellus, the measured emission rate from Barkley et al.[6] is directly used for upstream emission rate. While for processing emission rate, since there are no measurements covering processing stage in this region, we use the measurements data in southwestern Marcellus as approximation. The measured regional methane flux from Caulton et al.[24] is distributed among different stages with the processing stage 0.14%-0.79%, as shown in Table S35. Since the upper range of this emission range is surprisingly high, particularly because there were no major or widespread activities of which the authors are aware that are typically associated with high methane emission rates, the upper bound value of this emission rate range is removed. Therefore, the emission rate 0.14% is used for data in our model and lower bound of sensitivity. The upper bound of sensitivity analysis is set to be 1.5 times of 0.14%, as shown in Table S38.

In the Permian, the measured emission rate used in our LCA model for both upstream and processing are obtained from Zhang et al study,[8] which is obtained by allocating to different stages based on 2018 GHGRP reported methane emissions across production, gathering and boosting, and processing[12], as shown in Table S36. In sensitivity analysis, the measurements in Chen et al. study[37] is also included to represent the emission variability in Permian basin, as shown in Table S37. The lower and upper bound value are set to be minimum and maximum value of Zhang et al. and Chen et al. studies. The methane emission rate used in model and sensitivity analysis are shown in Table S38.

Table S38. Methane emission rate in model and sensitivity analysis

Basin	Parameter	Upstream	Source	Processing	Source
Northeastern Marcellus	Data in model	0.40%	Barkley et al. 2017	0.14%	Caulton et al. 2014
	Lower bound of sensitivity analysis	0.08%	Barkley et al. 2017	0.14%	Caulton et al. 2014
	Upper bound of sensitivity analysis	0.72%	Barkley et al. 2017	0.21%	1.5 times of data in model
Permian	Data in model	3.52%	Zhang et al. 2020	0.19%	Zhang et al. 2020
	Lower bound of sensitivity analysis	2.85%	Zhang et al. 2020	0.15%	Zhang et al. 2020

	Upper bound of sensitivity analysis	6.62%	Chen et al. 2022	0.34%	Chen et al. 2022

S 10. Life cycle GHG emission intensity under 20-year GWP

After the establishment of our LCA model, we calculated the GHG emissions along each LNG supply chain. Figure S5 show the GHG emissions along the LNG supply chain from Marcellus and Permian basins to UK and China under 20-year Global Warming Potential (GWP).

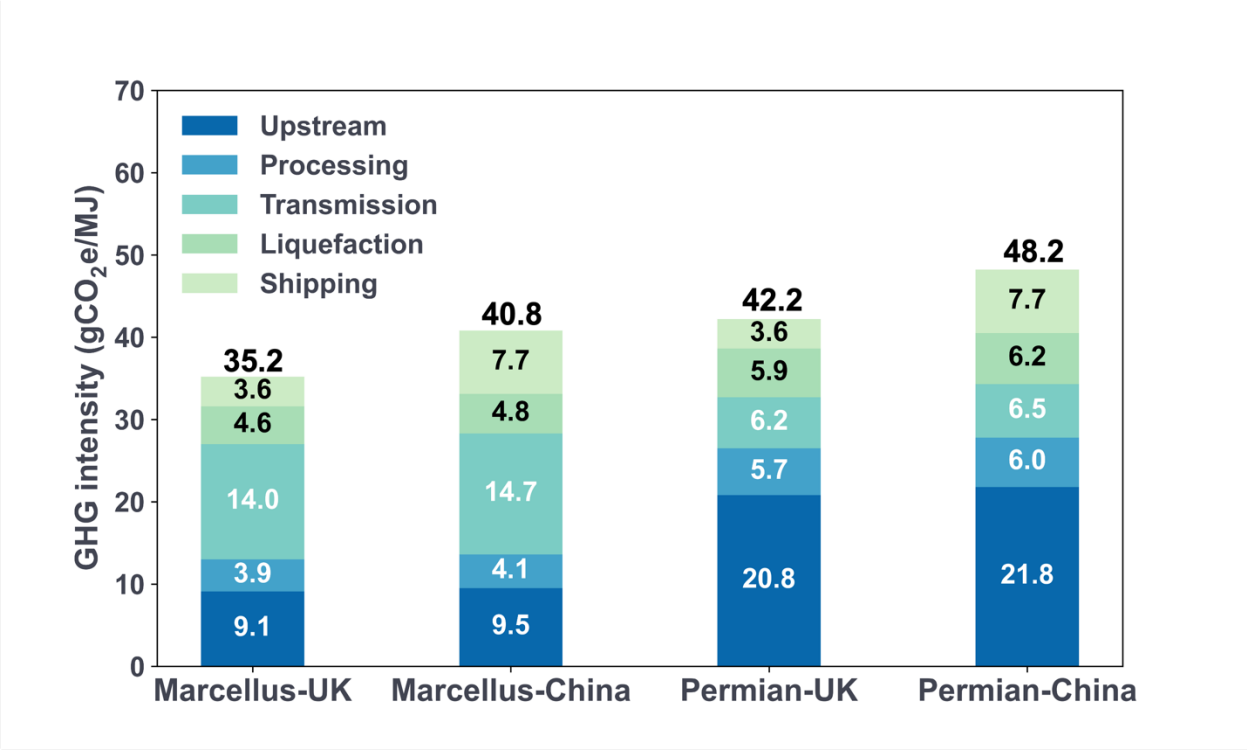

Figure S5. Emission intensity of LNG supply chain under 20-year GWP

S 11. Methane emission

Table S39 shows the methane and GHG emissions in Marcellus-UK and Permian-UK supply chains based on carbon dioxide equivalent by using methane 100-year GWP. Although methane and GHG emissions differ across different LNG supply chains, the contribution of methane to total GHG emissions at each stage is quite similar between Marcellus-UK and Permian-UK LNG supply chains.

In both Marcellus-UK and Permian-UK supply chains, the upstream and transmissions are two largest contributors to total methane emissions. In the Marcellus basin, the transmission and upstream stage

contribute 50% and 32% of total methane emissions along Marcellus-UK supply chain. The large contribution of transmission emission in Marcellus-UK supply chain is associated with long transmission distance between Marcellus processing plant to liquefaction facility. While in the Permian basin, the upstream stage is the largest contributor to total methane emissions, accounting for 68% in Permian-UK supply chain. The transmission stage contributes 17% of total methane emissions in Permian-UK supply chain.

Compared with methane emissions from upstream and transmission stages, the influence of methane emissions from other stages along both Marcellus-UK and Permian-UK supply chains are minor. The processing stages account for around 10% of the total methane emissions for both Marcellus-UK and Permian-UK supply chains. The contribution of methane emissions from liquefaction and shipping is minor, which is less than 10%.

Table S39. Methane emission from each stage of the Marcellus-UK and Permian-UK supply chains

Stage	**Marcellus-UK (steam)**			**Permian-UK (steam)**		
	CH_4 emission (gCO_2e/MJ LNG delivered)	**Total GHG emission (gCO_2e/MJ LNG delivered)**	**CH_4 emission/ Total GHG emission**	**CH_4 emission (gCO_2e/MJ LNG delivered)**	**Total GHG emission (gCO_2e/MJ LNG delivered)**	**CH_4 emission /Total GHG emission**
Upstream	3.00	4.81	62%	8.06	15.17	53%
Processing	0.99	2.48	40%	1.04	4.22	25%
Transmission	4.62	7.49	62%	2.03	3.35	61%
Liquefaction	0.04	4.53	1%	0.04	5.87	1%
Shipping	0.65	2.72	24%	0.65	2.72	24%
Total	9.29	22.02	42%	11.82	31.33	38%

Figure S6(a) shows the GHG emissions of each stage in the Marcellus-China and Permian-China supply chains before and after including measurement-informed emission intensity. The GHG emission difference at the upstream stage between Marcellus-China and Permian-China supply chains increased by 35% from 8.1 gCO_2e/(MJ LNG delivered) to 10.9 gCO_2e/(MJ LNG delivered). The GHG emission difference at the processing stage between these two supply chains are comparable before and after incorporating measurements.

The methane emissions in our model are divided into six categories, as shown in Figure S6(b). The area of the pie chart is proportional to the total methane emissions across each supply chain.

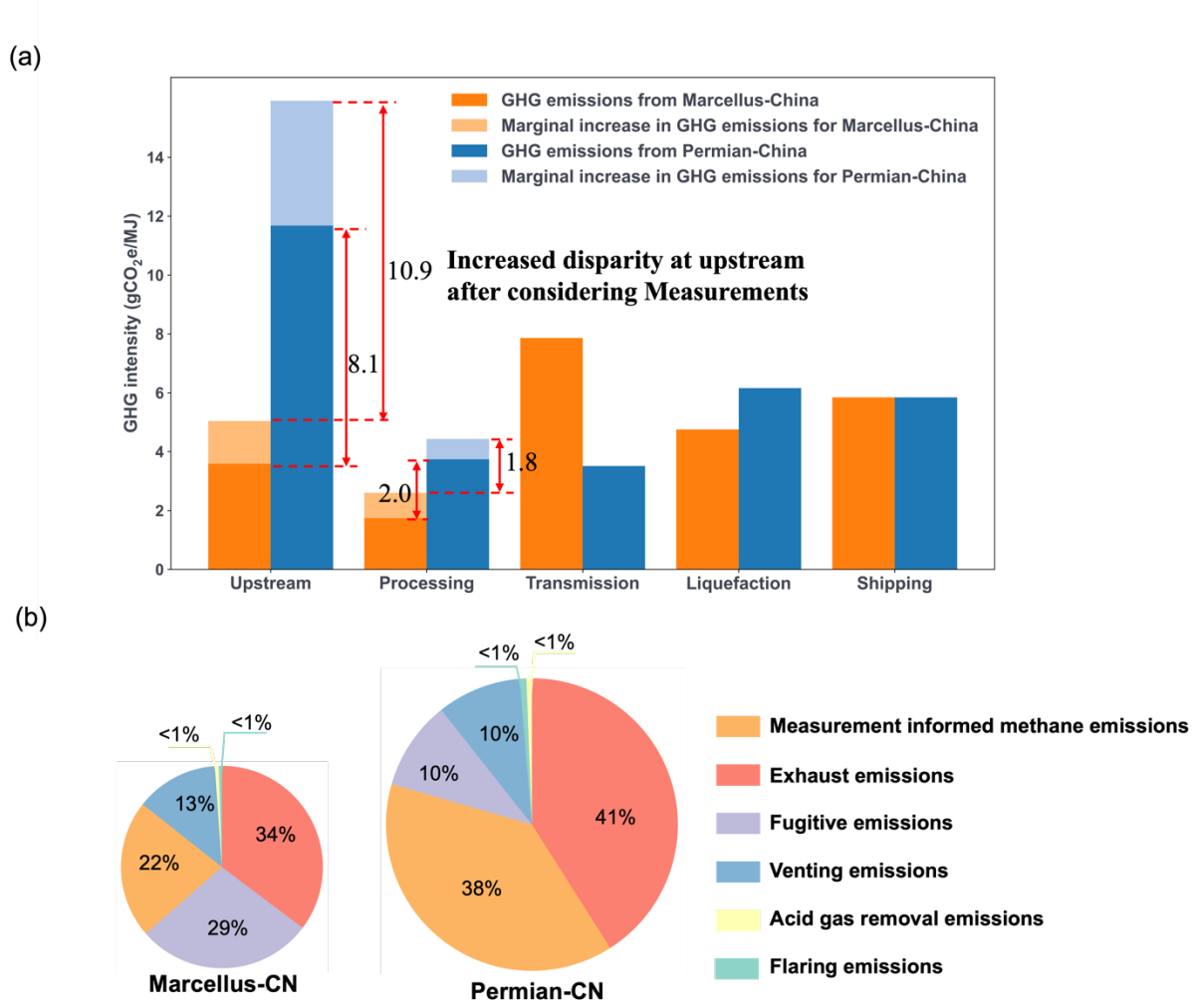

Figure S6. Impact of measurement-informed methane emission on supply chain emissions. (a) GHG emissions of each stage before and after considering the measurement-informed emissions estimates. The orange and blue bars represent the GHG emissions from Marcellus-China and Permian-China supply chains, respectively. The lighter color bars at the upstream and processing stage represent the marginal increase in emission intensity from the use of measurement-informed inventories (b) Contribution of each methane emission source in Marcellus-China and Permian-China LNG supply chains, respectively.

S 12. Comparison with other literature

The emission difference at the upstream stage between Roman-White et al. and our study has already been illustrated in the manuscript, here we continue to discuss the difference in processing, transmission, liquefaction, and shipping stages among the US-UK supply chain in Roman-White et al. study and Marcellus-UK and Permian-UK supply chains in our study. The GHG emissions of LNG supply chains in Roman-White et al. study and our study can be found in Figure 4 in the manuscript.

The GHG emission from the processing stage in Roman-White et al. is 3.3 gCO_2e/MJ, which is 0.8 gCO_2e/MJ higher and 0.9 gCO_2e/MJ lower than that of Marcellus-UK and Permian-UK supply chains, respectively. In their study, due to limited supplier participation, the US average profile extracted from GHGRP was used to represent the processing stage within the LNG supply chain. However, this national-average data masks the difference between regions. The higher degree of electrification in the Marcellus basin leads to less emission-intensive processing plant in that region compared to the Permian basin.

The transmission emission in Roman-White et al. study is slightly higher than that in the Permian-UK supply chain in our model. Because in our study, the calculated transmission emission assumes that all Permian natural gas is transported to the Sabine Pass Liquefaction facility, whereas in Roman-White et al. study, there are serval gas suppliers, some of which are located farther than the average Permian basin – SPL distance in our analysis. Thus, the higher emissions intensity is attributable to the longer pipeline gas transportation distance.

The GHG emissions from the liquefaction stage in the Permian-UK supply chain are similar to that in Roman-White et al. study and higher than that in the Marcellus-UK supply chain. The lower liquefaction GHG emissions in the Marcellus-UK supply chain are associated with the lower concentration of carbon dioxide that needs to be removed from Marcellus pipeline gas.

For the shipping stage, Roman-White et al. calculates the shipping emissions from the Sabine Pass terminal to the UK based on the 2018 voyage log and proprietary vessel data for cargo loaded with Cheniere SPL LNG in 2018. This shipping emission value is within the range of the emission results of 1.5-2.7 gCO_2/MJ (2.7 gCO_2/MJ is the shipping emission based on steam powered propulsion system; 1.5 gCO_2/MJ is shipping emission based on X-DF powered system) from the two different propulsion systems in our model.

S 13. Sensitivity analysis

In our study, we conducted sensitivity analysis for Marcellus-UK and Permian-UK supply chain separately. For each supply chain, we selected seven parameters, which highly influence the total GHG emission estimates and roughly cover all stages along the LNG supply chain. The parameters used in this analysis are summarized in Table S40. It should be noted that the lower and upper bound of venting & fugitives rate at transmission, and flaring emission at liquefaction are set to be 0.5 and 1.5 times the values in the base case to approximately represent the uncertainty range. In addition, we assume two emission allocation methods, the first one is to allocate the emission of each process to the products associated with the process according to heating content, and the second emission allocation method is to assign all the emissions of each stage to the LNG.

Table S40. Parameters for sensitivity analysis along Marcellus-UK and Permian-UK LNG supply chains

Parameters	Marcellus-UK			Permian-UK		
	Base case	Lower bound	Upper Bound	Base case	Lower bound	Upper Bound
Upstream measurement-informed emission rate	0.40%	0.08%	0.72%	3.52%	2.85%	6.62%
Processing measurement-informed emission rate	0.14%	0.14%	0.21%	0.19%	0.15%	0.34%
Venting & fugitives rate at transmission	0.42%	0.21%	0.63%	0.21%	0.11%	0.32%
Flaring emission at liquefaction	0.1450 gCO_2e/MJ	0.0725 gCO_2e/MJ	0.2175 gCO_2e/MJ	0.1450 gCO_2e/MJ	0.0725 gCO_2e/MJ	0.2175 gCO_2e/MJ
LNG tanker type	Steam powered with capacity 137,000 m^3	X-DF powered with capacity 180,000 m^3	Steam powered with capacity 137,000 m^3	Steam powered with capacity 137,000 m^3	X-DF powered with capacity 180,000 m^3	Steam powered with capacity 137,000 m^3
Shipping distance	4520 nm	4520 nm	9966 nm	4520 nm	4520 nm	9966 nm
Emission allocation method	Emission allocation based on heating content	Emission allocation based on heating content	Assign all the emission to LNG	Emission allocation based on heating content	Emission allocation based on heating content	Assign all the emission to LNG

References

(1) *Infrastructure Projects Connect Marcellus Shale To Ethane, NGL Markets*; The American Oil & Gas Reporter, 2011. https://www.aogr.com/magazine/cover-story/infrastructure-projects-connect-marcellus-shale-to-ethane-ngl-markets (accessed 2024-03-11).

(2) Mallapragada, D. S.; Reyes-Bastida, E.; Roberto, F.; McElroy, E. M.; Veskovic, D.; Laurenzi, I. J. Life Cycle Greenhouse Gas Emissions and Freshwater Consumption of Liquefied Marcellus Shale Gas Used for International Power Generation. *Journal of Cleaner Production* **2018**, *205*, 672–680. https://doi.org/10.1016/j.jclepro.2018.09.111.

(3) Littlefield, J.; Roman-White, S.; Augustine, D.; Pegallapati, A.; Zaimes, G. G.; Rai, S.; Cooney, G.; Skone, T. J. *LIFE CYCLE ANALYSIS OF NATURAL GAS EXTRACTION AND POWER GENERATION*; National Energy Technology Laboratory (NETL), 2019; p 374.

(4) Roman-White, S.; Rai, S.; Littlefield, J.; Cooney, G.; Skone, T. J. *LIFE CYCLE GREENHOUSE GAS PERSPECTIVE ON EXPORTING LIQUEFIED NATURAL GAS FROM THE UNITED STATES: 2019 UPDATE*; National Energy Technology Laboratory (NETL), 2019; p 54.
(5) Allen, D. T.; Torres, V. M.; Thomas, J.; Sullivan, D. W.; Harrison, M.; Hendler, A.; Herndon, S. C.; Kolb, C. E.; Fraser, M. P.; Hill, A. D.; Lamb, B. K.; Miskimins, J.; Sawyer, R. F.; Seinfeld, J. H. Measurements of Methane Emissions at Natural Gas Production Sites in the United States. *Proc. Natl. Acad. Sci. U.S.A.* **2013**, *110* (44), 17768–17773. https://doi.org/10.1073/pnas.1304880110.
(6) Barkley, Z. R.; Lauvaux, T.; Davis, K. J.; Deng, A.; Miles, N. L.; Richardson, S. J.; Cao, Y.; Sweeney, C.; Karion, A.; Smith, M.; Kort, E. A.; Schwietzke, S.; Murphy, T.; Cervone, G.; Martins, D.; Maasakkers, J. D. Quantifying Methane Emissions from Natural Gas Production in North-Eastern Pennsylvania. *Atmos. Chem. Phys.* **2017**, *17* (22), 13941–13966. https://doi.org/10.5194/acp-17-13941-2017.
(7) Oil and Gas Well Production in Pennsylvania. https://greenport.pa.gov/ReportExtracts/OG/Index (accessed 2024-02-29).
(8) Zhang, Y.; Gautam, R.; Pandey, S.; Omara, M.; Maasakkers, J. D.; Sadavarte, P.; Lyon, D.; Nesser, H.; Sulprizio, M. P.; Varon, D. J.; Zhang, R.; Houweling, S.; Zavala-Araiza, D.; Alvarez, R. A.; Lorente, A.; Hamburg, S. P.; Aben, I.; Jacob, D. J. Quantifying Methane Emissions from the Largest Oil-Producing Basin in the United States from Space. *Sci. Adv.* **2020**, *6* (17), eaaz5120. https://doi.org/10.1126/sciadv.aaz5120.
(9) *Monthly Summary of Texas Natural Gas*; Texas Railroad Commission (TRRC). https://www.rrc.texas.gov/oil-and-gas/research-and-statistics/production-data/monthly-summary-of-texas-natural-gas/ (accessed 2024-02-29).
(10) *Monthly Crude Oil Production.*; Texas Railroad Commission (TRRC). https://www.rrc.texas.gov/oil-and-gas/research-and-statistics/production-data/monthly-crude-oil-production-by-district-and-field/ (accessed 2024-02-29).
(11) *County Production and Injection by Month.*; New mexico Oil Conservation Division (NMOCD). https://wwwapps.emnrd.nm.gov/ocd/ocdpermitting/Reporting/Production/CountyProductionInjectionSummary.aspx (accessed 2024-02-29).
(12) Rosselot, K. S.; Allen, D. T.; Ku, A. Y. Comparing Greenhouse Gas Impacts from Domestic Coal and Imported Natural Gas Electricity Generation in China. *ACS Sustainable Chem. Eng.* **2021**, *9* (26), 8759–8769. https://doi.org/10.1021/acssuschemeng.1c01517.
(13) Adam, B. OPGEE_v2.0. https://eao.stanford.edu/research-project/opgee-oil-production-greenhouse-gas-emissions-estimator#:~:text=The%20Oil%20Production%20Greenhouse%20gas%20Emissions%20Estimator%20(OPGEE)%20is%20an,and%20transport%20of%20crude%20petroleum.
(14) Laurenzi, I. J.; Jersey, G. R. Life Cycle Greenhouse Gas Emissions and Freshwater Consumption of Marcellus Shale Gas. *Environ. Sci. Technol.* **2013**, *47* (9), 4896–4903. https://doi.org/10.1021/es305162w.
(15) Mallapragada, D. S.; Naik, I.; Ganesan, K.; Banerjee, R.; Laurenzi, I. J. Life Cycle Greenhouse Gas Impacts of Coal and Imported Gas-Based Power Generation in the Indian Context. *Environ. Sci. Technol.* **2019**, *53* (1), 539–549. https://doi.org/10.1021/acs.est.8b04539.

(16) *Inventory of U.S. Greenhouse Gas Emissions and Sinks, 1990-2016.*; U.S. Environmental Protection Agency. https://www.epa.gov/sites/default/files/2018-01/documents/2018_complete_report.pdf.
(17) Contreras, W.; Hardy, C.; Tovar, K.; Piwetz, A. M.; Harris, C. R.; Tullos, E. E.; Bymaster, A.; McMichael, J.; Laurenzi, I. J. Life Cycle Greenhouse Gas Emissions of Crude Oil and Natural Gas from the Delaware Basin. *Journal of Cleaner Production* **2021**, *328*, 129530. https://doi.org/10.1016/j.jclepro.2021.129530.
(18) EPA. GHGRP and Oil and Gas Industry | Greenhouse Gas Reporting Program (GHGRP) | US EPA. https://www.epa.gov/ghgreporting/ghgrp-and-oil-and-gas-industry.
(19) EPA. Greenhouse Gas Reporting Program (GHGRP). https://www.epa.gov/ghgreporting/data-sets.
(20) *Carbon Dioxide Emissions Coefficients by Fuel*; U.S. Energy Information Administration. https://www.eia.gov/environment/emissions/co2_vol_mass.php.
(21) *2017-2021 CO2, SO2 and NOx Emission Rates*; PJM interconnection LLC. https://pjm.com/-/media/library/reports-notices/special-reports/2021/2021-emissions-report.ashx (accessed 2024-03-05).
(22) Roman-White, S. A.; Littlefield, J. A.; Fleury, K. G.; Allen, D. T.; Balcombe, P.; Konschnik, K. E.; Ewing, J.; Ross, G. B.; George, F. LNG Supply Chains: A Supplier-Specific Life-Cycle Assessment for Improved Emission Accounting. *ACS Sustainable Chem. Eng.* **2021**, *9* (32), 10857−10867. https://doi.org/10.1021/acssuschemeng.1c03307.
(23) Zimmerle, D. J.; Williams, L. L.; Vaughn, T. L.; Quinn, C.; Subramanian, R.; Duggan, G. P.; Willson, B.; Opsomer, J. D.; Marchese, A. J.; Martinez, D. M.; Robinson, A. L. Methane Emissions from the Natural Gas Transmission and Storage System in the United States. *Environ. Sci. Technol.* **2015**, *49* (15), 9374−9383. https://doi.org/10.1021/acs.est.5b01669.
(24) Caulton, D. R.; Shepson, P. B.; Santoro, R. L.; Sparks, J. P.; Howarth, R. W.; Ingraffea, A. R.; Cambaliza, M. O. L.; Sweeney, C.; Karion, A.; Davis, K. J.; Stirm, B. H.; Montzka, S. A.; Miller, B. R. Toward a Better Understanding and Quantification of Methane Emissions from Shale Gas Development. *Proc. Natl. Acad. Sci. U.S.A.* **2014**, *111* (17), 6237−6242. https://doi.org/10.1073/pnas.1316546111.
(25) Understaning Natural Gas Compressor Stations. *PennState Extension*. https://extension.psu.edu/understanding-natural-gas-compressor-stations (accessed 2024-03-06).
(26) *Heat Content of Natural Gas Consumed*; U.S. Energy Information Administration. https://www.eia.gov/dnav/ng/ng_cons_heat_a_EPG0_VGTH_btucf_a.htm (accessed 2024-03-06).
(27) Nie, Y.; Zhang, S.; Liu, R. E.; Roda-Stuart, D. J.; Ravikumar, A. P.; Bradley, A.; Masnadi, M. S.; Brandt, A. R.; Bergerson, J.; Bi, X. T. Greenhouse-Gas Emissions of Canadian Liquefied Natural Gas for Use in China: Comparison and Synthesis of Three Independent Life Cycle Assessments. *Journal of Cleaner Production* **2020**, *258*, 120701. https://doi.org/10.1016/j.jclepro.2020.120701.
(28) Shipping Distance Calculator. http://www.shiptraffic.net/2001/05/sea-distances-calculator.html.
(29) Rosselot, K. S.; Balcombe, P.; Ravikumar, A. P.; Allen, D. T. Simulating the Variability of Methane and CO_2 Emissions from Liquefied Natural Gas Shipping: A Time-in-Mode and

Carrier Technology Approach. *ACS Sustainable Chem. Eng.* **2023**, *11* (43), 15632–15643. https://doi.org/10.1021/acssuschemeng.3c04269.
(30) Balcombe, P.; Heggo, D. A.; Harrison, M. Total Methane and CO_2 Emissions from Liquefied Natural Gas Carrier Ships: The First Primary Measurements. *Environ. Sci. Technol.* **2022**, *56* (13), 9632–9640. https://doi.org/10.1021/acs.est.2c01383.
(31) Rosselot, K. S.; Balcombe, P.; Ravikumar, A. P.; Allen, D. T. Simulating the Variability of Methane and CO_2 Emissions from Liquefied Natural Gas Shipping: A Time-in-Mode and Carrier Technology Approach. *ACS Sustainable Chem. Eng.* **2023**, *11* (43), 15632–15643. https://doi.org/10.1021/acssuschemeng.3c04269.
(32) Peischl, J.; Ryerson, T. B.; Aikin, K. C.; Gouw, J. A.; Gilman, J. B.; Holloway, J. S.; Lerner, B. M.; Nadkarni, R.; Neuman, J. A.; Nowak, J. B.; Trainer, M.; Warneke, C.; Parrish, D. D. Quantifying Atmospheric Methane Emissions from the Haynesville, Fayetteville, and Northeastern Marcellus Shale Gas Production Regions. *J. Geophys. Res. Atmos.* **2015**, *120* (5), 2119–2139. https://doi.org/10.1002/2014JD022697.
(33) Omara, M.; Sullivan, M. R.; Li, X.; Subramanian, R.; Robinson, A. L.; Presto, A. A. Methane Emissions from Conventional and Unconventional Natural Gas Production Sites in the Marcellus Shale Basin. *Environ. Sci. Technol.* **2016**, *50* (4), 2099–2107. https://doi.org/10.1021/acs.est.5b05503.
(34) Robertson, A. M.; Edie, R.; Field, R. A.; Lyon, D.; McVay, R.; Omara, M.; Zavala-Araiza, D.; Murphy, S. M. New Mexico Permian Basin Measured Well Pad Methane Emissions Are a Factor of 5–9 Times Higher Than U.S. EPA Estimates. *Environ. Sci. Technol.* **2020**, *54* (21), 13926–13934. https://doi.org/10.1021/acs.est.0c02927.
(35) Irakulis-Loitxate, I.; Guanter, L.; Liu, Y.-N.; Varon, D. J.; Maasakkers, J. D.; Zhang, Y.; Chulakadabba, A.; Wofsy, S. C.; Thorpe, A. K.; Duren, R. M.; Frankenberg, C.; Lyon, D. R.; Hmiel, B.; Cusworth, D. H.; Zhang, Y.; Segl, K.; Gorroño, J.; Sánchez-García, E.; Sulprizio, M. P.; Cao, K.; Zhu, H.; Liang, J.; Li, X.; Aben, I.; Jacob, D. J. Satellite-Based Survey of Extreme Methane Emissions in the Permian Basin. *Sci. Adv.* **2021**, *7* (27), eabf4507. https://doi.org/10.1126/sciadv.abf4507.
(36) Cusworth, D. H.; Duren, R. M.; Thorpe, A. K.; Olson-Duvall, W.; Heckler, J.; Chapman, J. W.; Eastwood, M. L.; Helmlinger, M. C.; Green, R. O.; Asner, G. P.; Dennison, P. E.; Miller, C. E. Intermittency of Large Methane Emitters in the Permian Basin. *Environ. Sci. Technol. Lett.* **2021**, *8* (7), 567–573. https://doi.org/10.1021/acs.estlett.1c00173.
(37) Chen, Y.; Sherwin, E. D.; Berman, E. S. F.; Jones, B. B.; Gordon, M. P.; Wetherley, E. B.; Kort, E. A.; Brandt, A. R. Quantifying Regional Methane Emissions in the New Mexico Permian Basin with a Comprehensive Aerial Survey. *Environ. Sci. Technol.* **2022**, *56* (7), 4317–4323. https://doi.org/10.1021/acs.est.1c06458.